Discontinuous Galerkin methods with staggered hybridization for linear elastodynamics

Eric T. Chung, Jie Du *, Chi Yeung Lam

Department of Mathematics, The Chinese University of Hong Kong, Hong Kong Special Administrative Region

ARTICLE INFO

ABSTRACT

In this paper, we will develop a new staggered hybridization technique for discontinuous Galerkin methods to discretize linear elastodynamic equations. The idea of hybridization is used extensively in many discontinuous Galerkin methods, but the idea of staggered hybridization is new. Our new approach offers several advantages, namely energy conservation, high-order optimal convergence, preservation of symmetry for the stress tensor, block diagonal mass matrices as well as low dispersion error. The key idea is to use two staggered hybrid variables to enforce the continuity of the velocity and the continuity of the normal component of the stress tensor on a staggered mesh. We prove the stability and the convergence of the proposed scheme in both the semi-discrete and the fully-discrete settings. Numerical results confirm the optimal rate of convergence and show that the method has a superconvergent property for dispersion. Furthermore, an application of this method to Rayleigh wave propagation is presented.

© 2017 Elsevier Ltd. All rights reserved.

1. Introduction

Accurate elastic wave simulations are of critical importance in a variety of geophysical applications. One popular class of methods is the staggered grid finite difference methods proposed by [1–3], which are very efficient for regular domains with flat interfaces or surfaces. However, it is not easy to apply these methods to domains with complex geometries or nonflat interfaces, which arise in more realistic applications. Recently, the discontinuous Galerkin (DG) method has become increasingly popular, due to its great flexibility for higher-order spatial approximations and its ability of computing on irregular domains. For instances, [4] demonstrated the *hp*-adaptivity for 3-D elastic wave with convolution perfectly matched layer, [5] developed *hp*-adaptivity schemes for elastic scattering, [6] designed a numerical scheme with efficient parallel implementation for 3-D wave propagation problem in coupled elastic–acoustic media, and [7] proposed a solution strategy for this problem using *hp*-adaptivity.

For a linear elastic material, wave propagation in the domain $\Omega \subset \mathbb{R}^d$ is governed by

$$\rho \frac{\partial^2 \mathbf{w}}{\partial t^2} - \operatorname{div} \mathbf{C} \boldsymbol{\varepsilon}(\mathbf{w}) = \mathbf{f} \quad \text{in } \Omega, \tag{1}$$

where $d = 2$ or 3, $\rho > 0$ is the mass density, $\mathbf{w}(t, \mathbf{x}) : [0, \infty) \times \Omega \to \mathbb{R}^d$ is the displacement, $\mathbf{C}$ is the stiffness tensor of the medium, $\boldsymbol{\varepsilon}(\mathbf{w}) = \frac{1}{2}(\nabla \mathbf{w} + \nabla \mathbf{w}^T)$ is the strain tensor and $\mathbf{f}$ is the external force. There are two commonly used formulations for the discretization. The *displacement–stress formulation* solves this problem in terms of the displacement and/or stress.

---

* Corresponding author.
  E-mail address: jdu@math.cuhk.edu.hk (J. Du).

Examples of DG method of this type, include the Internal Penalty Discontinuous Galerkin (IPDG) methods in [8–10]. In addition, [11] proposed a DG method of this type where the energy is conserved with a suitable choice of numerical fluxes.

On the other hand, the *velocity–stress formulation* or the *velocity–strain formulation* solves this problem in terms of the velocity and the stress or strain, resulting in a first-order system. The displacement can be recovered by integrating the velocity in time. A variety of semi-discrete DG methods have been proposed to solve this system, e.g. [4,6,12,13]. These methods use discontinuous elements to discretize the space with time-stepping to solve the system. To achieve higher accuracy in time, [14] introduced the ADER-DG method for two-dimensional isotropic elastic wave propagation, where the upwind flux and the ADER scheme in time are used to get the same order of accuracy in space and in time.

Recently, a new class of staggered DG (SDG) methods based on staggered meshes has been successfully developed for the first-order formulation of wave equations. In [15,16], the SDG method was proposed for the time-dependent acoustic wave equation. Note that the idea for the acoustic-wave equation cannot be directly applied to the elastic-wave equation due to the symmetry of the stress tensor. In [17], a new SDG method using the Lagrange multiplier technique for the enforcement of the symmetry of the stress tensor was constructed. However, due to the staggered continuity requirements on basis functions, this SDG method only gives a weak symmetry condition for the stress tensor.

In this paper, we introduce a new idea for elastic wave simulations. In particular, we will develop a new staggered hybridization technique. We remark that the idea of hybridization is used extensively in many discontinuous Galerkin methods, such as [13,18–22], but the idea of staggered hybridization is new. In our new method, the construction of a staggered mesh follows the ideas from [15,16,23], where SDG methods were proposed for the time-dependent acoustic wave equation and the static linear elastic equation. The new method is based on piecewise polynomial approximations. Compared to [17], the continuity requirements on basis functions are removed, and the symmetry of the stress tensor is strongly enforced in the approximation space. To couple the basis functions across element boundaries, two staggered hybrid variables are used. These two hybrid variables are defined on edges of the staggered mesh, and are used to enforce the continuity of the velocity and the continuity of the normal component of the stress tensor in a staggered way. The resulting scheme offers several advantages, namely energy conservation, high-order optimal convergence as well as low dispersion error. Moreover, the new scheme preserves the strong symmetry for the stress tensor. With respect to the time-stepping, the new scheme requires only solutions of local saddle point problems defined on unions of few elements, and is thus very efficient. This "local" feature is the result of our staggered hybridization. In addition, our method is locking-free. In other words, the convergence is independent of the first Lamé's parameter λ. For nearly incompressible materials, λ is very large and many standard methods fail to address these materials as the numerical error grows as λ increases. We remark that [17,24] show that the SDG scheme produces numerical solutions with dispersion errors that are two order higher than non-staggered DG schemes. We will show numerically that the new scheme proposed in this paper also has a high order dispersion error. We will also show an application involving the simulations of the Rayleigh waves.

The rest of this paper is organized as follows. The paper starts with the problem setting in Section 2. It is followed by the detail of the proposed method in Section 3. Next, analyses for the convergence, the conservation, and the stability of the semi-discrete solutions are given in Section 4. Analyses for fully discrete solutions are given in Section 5. Numerical examples are given in Section 6 to demonstrate the performance of the proposed method. Finally, in Section 7, we give some conclusions.

2. Problem setting

Denote the velocity $\mathbf{u} := \mathbf{w}_t$, the $d \times d$ stress tensor $\boldsymbol{\sigma} := \mathbf{C}\boldsymbol{\varepsilon}(\mathbf{w})$ and the compliance tensor $\mathbf{A} := \mathbf{C}^{-1}$. We rewrite (1) as the following first order system,

$$\rho \frac{\partial \mathbf{u}}{\partial t} - \operatorname{div} \boldsymbol{\sigma} = \mathbf{f}, \tag{2}$$

$$\mathbf{A} \frac{\partial \boldsymbol{\sigma}}{\partial t} - \boldsymbol{\varepsilon}(\mathbf{u}) = \mathbf{0}, \tag{3}$$

in a bounded domain $\Omega \subset \mathbf{R}^d$ ($d = 2, 3$) with a Lipschitz boundary. We consider the time t that lies in the interval $[0, T]$.

To fix the notation, we write $\mathbf{u} := (u_1, \ldots, u_d)^T$, $\boldsymbol{\sigma} := (\sigma_{ij})$ and $\mathbf{f} := (f_1, \ldots, f_d)^T$. We let $\boldsymbol{\sigma}_i$ be the ith row of $\boldsymbol{\sigma}$ and define the divergence as $\operatorname{div}\boldsymbol{\sigma} := (\operatorname{div}\boldsymbol{\sigma}_1, \ldots, \operatorname{div}\boldsymbol{\sigma}_d)^T$. Moreover, $\boldsymbol{\varepsilon}(\mathbf{u}) = \frac{1}{2}(\nabla \mathbf{u} + \nabla \mathbf{u}^T)$ is a symmetric matrix, where $\nabla \mathbf{u} := (\partial_j u_i)$ is the row-wise gradient of $\mathbf{u}$.

In the rest of this paper, we assume the elastic medium is homogeneous and isotropic. In other words, the compliance tensor $\mathbf{A}$ is given by

$$\mathbf{A}\boldsymbol{\tau} := \frac{1}{2\mu} \left(\boldsymbol{\tau} - \frac{\lambda}{2\mu + d\lambda} \operatorname{tr}(\boldsymbol{\tau}) \mathbf{I} \right), \tag{4}$$

where λ and μ are positive constants called the first and the second Lamé's parameters, respectively, $\operatorname{tr}(\boldsymbol{\tau})$ is the trace of $\boldsymbol{\tau}$ and $\mathbf{I}$ is the identity tensor.
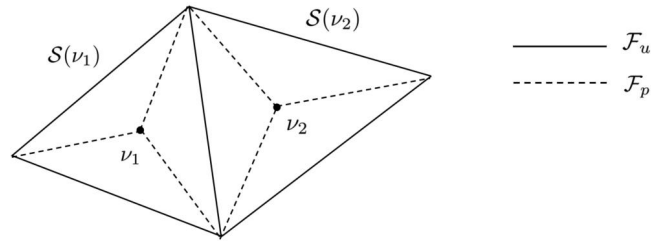
Fig. 1. An illustration of the staggered mesh in $\mathbb{R}^2$.

We assume the initial and boundary conditions for $\mathbf{u}$ and $\boldsymbol{\sigma}$ as

$$\mathbf{u}(0, \mathbf{x}) = \mathbf{u}_0(\mathbf{x}), \quad \mathbf{x} \in \Omega, \tag{5}$$

$$\boldsymbol{\sigma}(0, \mathbf{x}) = \boldsymbol{\sigma}_0(\mathbf{x}), \quad \mathbf{x} \in \Omega, \tag{6}$$

$$\mathbf{u}(t, \mathbf{x}) = \mathbf{u}_b(t, \mathbf{x}), \quad t \in (0, T], \; \mathbf{x} \in \partial\Omega_D, \tag{7}$$

$$\boldsymbol{\sigma}(t, \mathbf{x})\mathbf{n} = \boldsymbol{\sigma}_b(t, \mathbf{x}), \; t \in (0, T], \; \mathbf{x} \in \partial\Omega_N, \tag{8}$$

where $\partial\Omega_D$ is the Dirichlet boundary and $\partial\Omega_N = \partial\Omega \setminus \partial\Omega_D$ is the Neumann boundary. Here $\mathbf{n}$ is the outward unit normal vector on the boundary. The target is to compute approximations for $\mathbf{u}$ and $\boldsymbol{\sigma}$.

3. Numerical scheme

In this section, we show the detailed formulations of our scheme. The semi-discrete formulation is shown in Section 3.1 and the fully-discrete formulation is shown in Section 3.2.

3.1. The semi-discrete system

To derive the numerical scheme, we construct a *staggered mesh*. We follow the construction in [16]. To begin with, we triangulate the domain $\Omega \subset \mathbb{R}^d$ into a family of shape-regular d-simplices $\mathcal{T}_1$ without hanging nodes.

Then we form the staggered mesh by further division of the triangles. We illustrate the division in Fig. 1 for the two-dimensional case.

Let $\mathcal{F}_u$ be the set of all faces in $\mathcal{T}_1$, as illustrated by solid lines in Fig. 1. We further denote $\mathcal{F}_u^0 \subset \mathcal{F}_u$ as the set of all interior faces. Now for each simplex in $\mathcal{T}_1$, we pick an interior point ν and subdivide the simplex into $d+1$ sub-simplices by connecting ν to the vertices of the simplex. The union of these $d+1$ sub-simplices is called $\mathcal{S}(\nu)$. We introduce $\mathcal{N}$ to denote the set of all such interior points ν. Let $\mathcal{T}$ be the set of all these sub-simplices. As illustrated by dotted lines in Fig. 1, we use $\mathcal{F}_p$ to denote the set of all new faces formed in the subdivision process. Then we define $\mathcal{F}$ to be the set of all edges of $\mathcal{T}$, and thus we have $\mathcal{F} = \mathcal{F}_u \cup \mathcal{F}_p$. For each $\kappa \in \mathcal{F}_u$ we define $\mathcal{R}(\kappa)$ to be the union of simplices in $\mathcal{T}$ having the face κ. The regions $\mathcal{S}(\nu)$ and $\mathcal{R}(\kappa)$ form the staggered mesh.

Then we define some operators on the staggered mesh. For each element $\tau \in \mathcal{T}$, we define $\mathbf{n}_\tau$ as the outward unit normal vector on $\partial\tau$. We will simply use $\mathbf{n}$ instead of $\mathbf{n}_\tau$ if there is no confusion. For each face $e \in \mathcal{F}$, we define $\mathbf{n}_e$ in the following way. If $e \in \partial\Omega$, then we define $\mathbf{n}_e$ as the unit normal vector pointing outside of Ω. For an interior edge e with $e = \partial\tau^+ \cap \partial\tau^-$, we fix $\mathbf{n}_e$ as one of $\mathbf{n}_{\tau^+}$ and $\mathbf{n}_{\tau^-}$. We use notations $\mathbf{v}^+$ and $\mathbf{v}^-$ to denote the values of a vector $\mathbf{v}$ on e taken from τ^+ and τ^-, respectively. Then the jump of $\mathbf{v}$ over the face e is defined as

$$[\mathbf{v}]|_e := (\mathbf{n}_{\tau^-} \cdot \mathbf{n}_e)\mathbf{v}^- + (\mathbf{n}_{\tau^+} \cdot \mathbf{n}_e)\mathbf{v}^+.$$

Similarly, we use notations $\boldsymbol{\alpha}^+$ and $\boldsymbol{\alpha}^-$ to denote the values of a tensor $\boldsymbol{\alpha}$ on e taken from τ^+ and τ^-, respectively. The jump of the normal flux of $\boldsymbol{\alpha}$ is defined as

$$[\boldsymbol{\alpha}\mathbf{n}]|_e = \boldsymbol{\alpha}^+\mathbf{n}_{\tau^+} + \boldsymbol{\alpha}^-\mathbf{n}_{\tau^-}.$$

Next, we describe the finite element spaces. Let us denote $\mathcal{F}_u^D = \mathcal{F}_u^0 \cup \partial\Omega_D$ and $\mathcal{F}_p^N = \mathcal{F}_p \cup \partial\Omega_N$. Hence, $\mathcal{F} = \mathcal{F}_u^D \cup \mathcal{F}_p^N$. Moreover, we denote $P^k(\tau)$ and $P^k(e)$ as spaces of polynomials of degree at most k defined on the simplex τ and face e, respectively. Next, we introduce the finite element space of piecewise polynomials U_h, the space of $d \times d$ symmetric matrices W_h, and the spaces for the hybrid variables $\widehat{U}_h$ and $\widehat{W}_h$ as follows:

$$U_h := \{v : v|_\tau \in P^k(\tau), \; \forall \tau \in \mathcal{T}\},$$

$$W_h := \{\boldsymbol{\alpha} : \boldsymbol{\alpha}|_\tau \in [P^k(\tau)]^{d \times d}, \; \boldsymbol{\alpha} = \boldsymbol{\alpha}^T, \; \forall \tau \in \mathcal{T}\},$$

$$\widehat{U}_h := \{\widehat{v} : \widehat{v}|_e \in P^k(e), \; \forall e \in \mathcal{F}_p^N\},$$

$$\widehat{W}_h := \{\widehat{\boldsymbol{\alpha}} : \widehat{\boldsymbol{\alpha}}|_e \in P^k(e), \; \forall e \in \mathcal{F}_u^D\}.$$

We approximate solutions $\mathbf{u}$ and $\boldsymbol{\sigma}$ with $\mathbf{u}_h \in U_h^d$ and $\boldsymbol{\sigma}_h \in W_h$, respectively. Moreover, we approximate $\mathbf{u}|_{\mathcal{F}_p^N}$ and $\boldsymbol{\sigma}\mathbf{n}_e|_{\mathcal{F}_u^D}$ with $\widehat{\mathbf{u}}_h \in \widehat{U}_h^d$ and $\widehat{\boldsymbol{\sigma}}_h \in \widehat{W}_h^d$, respectively. By the definition of W_h, we know that the stress tensor $\boldsymbol{\sigma}_h$ is always strongly symmetric.

Note that in traditional SDG methods, we usually impose staggered continuities of $\mathbf{u}_h$ and $\boldsymbol{\sigma}_h\mathbf{n}_e$ in the definition of finite element spaces. However, it is not easy to construct basis functions in those spaces, especially when $\boldsymbol{\sigma}_h$ need to be strongly symmetric. In our new SDG method, functions in U_h and W_h can be discontinuous over element faces. Hence, it is very easy to construct basis functions. Instead of the definition of finite element spaces, we impose the continuity of $\mathbf{u}_h$ on $\mathcal{F}_u^D$ and the continuity of $\boldsymbol{\sigma}_h\mathbf{n}_e$ on $\mathcal{F}_p^N$ by the following conditions

$$\int_e [\mathbf{u}_h] \cdot \widehat{\boldsymbol{\alpha}}_h ds = 0, \qquad \forall \widehat{\boldsymbol{\alpha}}_h \in \widehat{W}_h^d, \ \forall e \in \mathcal{F}_u^D, \tag{9}$$

$$\int_e [\boldsymbol{\sigma}_h\mathbf{n}] \cdot \widehat{\mathbf{v}}_h ds = 0, \qquad \forall \widehat{\mathbf{v}}_h \in \widehat{U}_h^d, \ \forall e \in \mathcal{F}_p^N. \tag{10}$$

Note that on the boundary $e \in \partial\Omega_D$, we take $\mathbf{u}_b$ as the value of $\mathbf{u}_h$ taken from the outside of Ω. Also, we use $\boldsymbol{\sigma}_b$ as the value of $\boldsymbol{\sigma}_h\mathbf{n}_e$ on $e \in \partial\Omega_N$ taken from the outside of Ω. Hence, by the above continuity conditions, $\mathbf{u}_h|_{\partial\Omega_D}$ and $\boldsymbol{\sigma}_h\mathbf{n}_e|_{\partial\Omega_N}$ are just L_2 projections of the given boundary conditions.

To derive the SDG method, we multiply Eq. (2) with a smooth function $\mathbf{v}$ and multiply Eq. (3) with a test function $\boldsymbol{\alpha}$, and then integrate these two equations on each $\tau \in \mathcal{T}$. Integration by parts yields,

$$\int_\tau \rho \frac{\partial \mathbf{u}}{\partial t} \cdot \mathbf{v}dx + \int_\tau \boldsymbol{\sigma} : \nabla\mathbf{v}dx - \int_{\partial\tau} \boldsymbol{\sigma}\mathbf{n} \cdot \mathbf{v}ds = \int_\tau \mathbf{f} \cdot \mathbf{v}dx, \tag{11}$$

$$\int_\tau \mathbf{A} \frac{\partial \boldsymbol{\sigma}}{\partial t} : \boldsymbol{\alpha}dx + \int_\tau \mathbf{u} \cdot \text{div}\boldsymbol{\alpha}dx - \int_{\partial\tau} \mathbf{u} \cdot (\boldsymbol{\alpha}\mathbf{n})ds = 0, \tag{12}$$

for the solutions $\mathbf{u}$ and $\boldsymbol{\sigma}$.

Then we replace $\mathbf{u}$ and $\boldsymbol{\sigma}$ by the approximate solutions and use the test functions in the corresponding finite element spaces. We have, for any $\tau \in \mathcal{T}$, $\mathbf{v}_h \in U_h^d$ and $\boldsymbol{\alpha}_h \in W_h$,

$$\int_\tau \rho \frac{\partial \mathbf{u}_h}{\partial t} \cdot \mathbf{v}_h dx + \int_\tau \boldsymbol{\sigma}_h : \nabla\mathbf{v}_h dx - \int_{\partial\tau \cap \mathcal{F}_p^N} (\boldsymbol{\sigma}_h\mathbf{n}) \cdot \mathbf{v}_h ds - \int_{\partial\tau \cap \mathcal{F}_u^D} (\mathbf{n} \cdot \mathbf{n}_e)\widehat{\boldsymbol{\sigma}}_h \cdot \mathbf{v}_h ds = \int_\tau \mathbf{f} \cdot \mathbf{v}_h dx, \tag{13}$$

$$\int_\tau \mathbf{A} \frac{\partial \boldsymbol{\sigma}_h}{\partial t} : \boldsymbol{\alpha}_h dx + \int_\tau \mathbf{u}_h \cdot \text{div}\,\boldsymbol{\alpha}_h dx - \int_{\partial\tau \cap \mathcal{F}_u^D} \mathbf{u}_h \cdot (\boldsymbol{\alpha}_h\mathbf{n})ds - \int_{\partial\tau \cap \mathcal{F}_p^N} \widehat{\mathbf{u}}_h \cdot (\boldsymbol{\alpha}_h\mathbf{n})ds = 0. \tag{14}$$

Note that although $\mathbf{u}_h$ and $\boldsymbol{\sigma}_h$ are just piecewise polynomials, the boundary terms in above formulations are actually well defined because of the continuity conditions (9) and (10).

Summing Eqs. (13) and (14) over all triangles $\tau \in \mathcal{T}$, we arrive at our SDG formulation: Find the unique solutions $\mathbf{u}_h = \mathbf{u}_h(t) \in U_h^d$, $\boldsymbol{\sigma}_h = \boldsymbol{\sigma}_h(t) \in W_h$, $\widehat{\mathbf{u}}_h = \widehat{\mathbf{u}}_h(t) \in \widehat{U}_h^d$, and $\widehat{\boldsymbol{\sigma}}_h = \widehat{\boldsymbol{\sigma}}_h(t) \in \widehat{W}_h^d$ such that for all test functions $\mathbf{v}_h \in U_h^d$, $\boldsymbol{\alpha}_h \in W_h, \widehat{\mathbf{v}}_h \in \widehat{U}_h^d$ and $\widehat{\boldsymbol{\alpha}}_h \in \widehat{W}_h^d$,

$$\int_\Omega \rho \frac{\partial \mathbf{u}_h}{\partial t} \cdot \mathbf{v}_h dx + B(\boldsymbol{\sigma}_h, \mathbf{v}_h) - D^*(\widehat{\boldsymbol{\sigma}}_h, \mathbf{v}_h) = \int_\Omega \mathbf{f} \cdot \mathbf{v}_h dx, \tag{15}$$

$$\int_\Omega \mathbf{A} \frac{\partial \boldsymbol{\sigma}_h}{\partial t} : \boldsymbol{\alpha}_h dx - B^*(\mathbf{u}_h, \boldsymbol{\alpha}_h) + D(\widehat{\mathbf{u}}_h, \boldsymbol{\alpha}_h) = 0, \tag{16}$$

$$D^*(\widehat{\boldsymbol{\alpha}}_h, \mathbf{u}_h) = 0, \tag{17}$$

$$D(\widehat{\mathbf{v}}_h, \boldsymbol{\sigma}_h) = 0, \tag{18}$$

where

$$B(\boldsymbol{\alpha}, \mathbf{v}) := \int_\Omega \boldsymbol{\alpha} : \nabla\mathbf{v}dx - \sum_{e \in \mathcal{F}_p^N} \int_e [\boldsymbol{\alpha}\mathbf{n} \cdot \mathbf{v}]ds,$$

$$B^*(\mathbf{v}, \boldsymbol{\alpha}) := -\int_\Omega \mathbf{v} \cdot \text{div}\,\boldsymbol{\alpha}dx + \sum_{e \in \mathcal{F}_u^D} \int_e [\boldsymbol{\alpha}\mathbf{n} \cdot \mathbf{v}]ds,$$

$$D^*(\widehat{\boldsymbol{\alpha}}, \mathbf{v}) := \sum_{e \in \mathcal{F}_u^D} \int_e \widehat{\boldsymbol{\alpha}} \cdot [\mathbf{v}]ds,$$

$$D(\widehat{\mathbf{v}}, \boldsymbol{\alpha}) := -\sum_{e \in \mathcal{F}_p^N} \int_e \widehat{\mathbf{v}} \cdot [\boldsymbol{\alpha}\mathbf{n}]ds.$$

Here, $[\boldsymbol{\alpha}\mathbf{n} \cdot \mathbf{v}]|_e := (\boldsymbol{\alpha}^-\mathbf{n}_{\tau^-}) \cdot \mathbf{v}^- + (\boldsymbol{\alpha}^+\mathbf{n}_{\tau^+}) \cdot \mathbf{v}^+$.

3.2. The fully discrete system

In this section, we consider the fully discrete system, in which both time and space are discretized. Let Δt be the time step. To simplify the notation, we denote $\mathbf{x}^\ell$ to be $\mathbf{x}(\ell\Delta t, \cdot)$, i.e. the variable $\mathbf{x}$ at the ℓ-th time step. We define the discrete time derivative operator by

$$\delta_t \mathbf{x}^\ell := \frac{1}{\Delta t}(\mathbf{x}^{\ell+\frac{1}{2}} - \mathbf{x}^{\ell-\frac{1}{2}}),$$

where $\mathbf{x}$ can be $\mathbf{u}_h, \boldsymbol{\sigma}_h, \widehat{\mathbf{u}}_h$ and $\widehat{\boldsymbol{\sigma}}_h$.

We will apply the standard leap-frog scheme. We compute $\mathbf{u}_h$ and $\widehat{\boldsymbol{\sigma}}_h$ at times $n\Delta t$, and compute $\boldsymbol{\sigma}_h, \widehat{\mathbf{u}}_h$ at times $(n+\frac{1}{2})\Delta t$. Using the discrete time derivative operator and following the scheme (15)–(18), we have

$$\int_\Omega \rho \delta_t \mathbf{u}_h^{n+\frac{1}{2}} \cdot \mathbf{v}_h dx + B(\boldsymbol{\sigma}_h^{n+\frac{1}{2}}, \mathbf{v}_h) - \frac{1}{2} D^* \left(\widehat{\boldsymbol{\sigma}}_h^n + \widehat{\boldsymbol{\sigma}}_h^{n+1}, \mathbf{v}_h\right) = \int_\Omega \mathbf{f}^{n+\frac{1}{2}} \cdot \mathbf{v}_h dx, \tag{19}$$

$$\int_\Omega \boldsymbol{A}\delta_t \boldsymbol{\sigma}_h^{n+1} : \boldsymbol{\alpha}_h dx - B^*(\mathbf{u}_h^{n+1}, \boldsymbol{\alpha}_h) + \frac{1}{2} D \left(\widehat{\mathbf{u}}_h^{n+\frac{1}{2}} + \widehat{\mathbf{u}}_h^{n+\frac{3}{2}}, \boldsymbol{\alpha}_h\right) = 0, \tag{20}$$

$$D^*(\widehat{\boldsymbol{\alpha}}_h, \mathbf{u}_h^{n+1}) = 0, \tag{21}$$

$$D(\widehat{\mathbf{v}}_h, \boldsymbol{\sigma}_h^{n+\frac{3}{2}}) = 0. \tag{22}$$

We initialize the system by taking $\mathbf{u}_h^0$ and $\boldsymbol{\sigma}_h^{\frac{1}{2}}$ as L^2 projection of $\mathbf{u}(0, \cdot)$ and $\boldsymbol{\sigma}(\frac{1}{2}\Delta t, \cdot)$, respectively. For $\boldsymbol{\sigma}(\frac{1}{2}\Delta t, \cdot)$, one can obtain its value by using a Taylor expansion at the initial time. Moreover, we take $\widehat{\mathbf{u}}_h^{\frac{1}{2}} = \widehat{\boldsymbol{\sigma}}_h^0 = \mathbf{0}$.

Next, we write down the linear system explicitly. We denote the dimensions of $U_h^d, W_h, \widehat{U}_h^d$, and $\widehat{W}_h^d$ by $m_U, m_W, m_{\widehat{U}}$, and $m_{\widehat{W}}$ respectively and let the basis functions of these spaces as $\{\mathbf{v}_i\}_{i=1}^{m_U}, \{\boldsymbol{\alpha}_i\}_{i=1}^{m_W}, \{\widehat{\mathbf{v}}_i\}_{i=1}^{m_{\widehat{U}}}$ and $\{\widehat{\boldsymbol{\alpha}}_i\}_{i=1}^{m_{\widehat{W}}}$ respectively. Then we can write

$$\mathbf{u}_h := \sum_{i=1}^{m_U} u_i \mathbf{v}_i, \qquad \boldsymbol{\sigma}_h := \sum_{i=1}^{m_W} \sigma_i \boldsymbol{\alpha}_i,$$

$$\widehat{\mathbf{u}}_h := \sum_{i=1}^{m_{\widehat{U}}} \widehat{u}_i \widehat{\mathbf{v}}_i \qquad \widehat{\boldsymbol{\sigma}}_h := \sum_{i=1}^{m_{\widehat{W}}} \widehat{\sigma}_i \widehat{\boldsymbol{\alpha}}_i.$$

Moreover, we denote $\vec{\mathbf{u}}_h := (u_1, \ldots, u_{m_U})^T, \vec{\boldsymbol{\sigma}}_h := (\sigma_1, \ldots, \sigma_{m_W})^T, \vec{\widehat{\mathbf{u}}}_h := (\widehat{u}_1, \ldots, \widehat{u}_{m_{\widehat{U}}})^T, \vec{\widehat{\boldsymbol{\sigma}}}_h := (\widehat{\sigma}_1, \ldots, \widehat{\sigma}_{m_{\widehat{W}}})^T$, and $\vec{\mathbf{f}} := (\int_\Omega \mathbf{f} \cdot \mathbf{v}_1 \, dx, \ldots, \int_\Omega \mathbf{f} \cdot \mathbf{v}_{m_U} \, dx)^T$. Next, we define two mass matrices:

$$(\mathbf{M}_u) := \int_\Omega \rho \mathbf{v}_j \cdot \mathbf{v}_i \, dx, \qquad (\mathbf{M}_\sigma) := \int_\Omega \boldsymbol{A}\boldsymbol{\alpha}_j : \boldsymbol{\alpha}_i \, dx.$$

We also define matrices that involve two spaces:

$$(\mathbf{B}_h)_{ij} := B(\boldsymbol{\alpha}_j, \mathbf{v}_i), \qquad \left(\mathbf{B}_h^*\right)_{ij} := B^*(\mathbf{v}_j, \boldsymbol{\alpha}_i),$$

$$\left(\mathbf{D}_h^*\right)_{ij} := D^*(\widehat{\boldsymbol{\alpha}}_j, \mathbf{v}_i), \qquad (\mathbf{D}_h)_{ij} := D(\widehat{\mathbf{v}}_j, \boldsymbol{\alpha}_i).$$

By integration by parts, we know that $B^*(\mathbf{v}_j, \boldsymbol{\alpha}_i) = B(\boldsymbol{\alpha}_i, \mathbf{v}_j)$, and hence $\mathbf{B}_h^* = \mathbf{B}_h^T$. Using the above notations, we write the fully discrete system (19)–(22) as

$$\frac{1}{\Delta t}\mathbf{M}_u \vec{\mathbf{u}}_h^{n+1} - \frac{1}{2}\mathbf{D}_h^* \vec{\widehat{\boldsymbol{\sigma}}}_h^{n+1} = \frac{1}{\Delta t}\mathbf{M}_u \vec{\mathbf{u}}_h^n + \frac{1}{2}\mathbf{D}_h^* \vec{\widehat{\boldsymbol{\sigma}}}_h^n - \mathbf{B}_h \vec{\boldsymbol{\sigma}}_h^{n+\frac{1}{2}} + \vec{\mathbf{f}}^{n+\frac{1}{2}}, \tag{23}$$

$$\frac{1}{\Delta t}\mathbf{M}_\sigma \vec{\boldsymbol{\sigma}}_h^{n+\frac{3}{2}} + \frac{1}{2}\mathbf{D}_h \vec{\widehat{\mathbf{u}}}_h^{n+\frac{3}{2}} = \frac{1}{\Delta t}\mathbf{M}_\sigma \vec{\boldsymbol{\sigma}}_h^{n+\frac{1}{2}} - \frac{1}{2}\mathbf{D}_h \vec{\widehat{\mathbf{u}}}_h^{n+\frac{1}{2}} + \mathbf{B}_h^T \vec{\mathbf{u}}_h^{n+1}, \tag{24}$$

$$(\mathbf{D}_h^*)^T \vec{\mathbf{u}}_h^{n+1} = \mathbf{0}, \tag{25}$$

$$(\mathbf{D}_h)^T \vec{\boldsymbol{\sigma}}_h^{n+\frac{3}{2}} = \mathbf{0}. \tag{26}$$

It is worth to note that the finite element spaces are defined locally and hence matrices $\mathbf{M}_u$ and $\mathbf{M}_\sigma$ are both block diagonal. Thus, we can compute $\vec{\mathbf{u}}_h^{n+1}$ and $\vec{\widehat{\boldsymbol{\sigma}}}_h^{n+1}$ locally on each $\mathcal{R}(e)$, $e \in \mathcal{F}_u$ by solving (23) and (25). Also, we can compute $\vec{\boldsymbol{\sigma}}_h^{n+\frac{3}{2}}$ and $\vec{\widehat{\mathbf{u}}}_h^{n+\frac{3}{2}}$ locally on each $\mathcal{S}(\nu)$, $\nu \in \mathcal{N}$ by solving (24) and (26). Hence, the scheme can be solved very efficiently.

4. Analysis for semi-discrete solutions

In this section, we will prove the stability, the wave energy conservation, and the optimal convergence of our scheme. For simplicity, we assume $\partial \Omega_D = \partial \Omega$ and $\mathbf{u}_b = \mathbf{0}$. However, our proof can be extended to the general case.

Although $\mathbf{u}_h$ and $\boldsymbol{\sigma}_h$ are both piecewise polynomials, since we compose staggered continuity conditions on numerical solutions, by denoting

$$U_c := \{v : v|_\tau \in P^k(\tau), \forall \tau \in \mathcal{T}, v \text{ is continuous on } e \in \mathcal{F}_u^0, v|_{\partial\Omega} = 0\},$$
$$W_c := \{\boldsymbol{\alpha} : \boldsymbol{\alpha}|_\tau \in [P^k(\tau)]^d, \forall \tau \in \mathcal{T}, \boldsymbol{\alpha} \cdot \mathbf{n}_e \text{ is continuous on } e \in \mathcal{F}_p\},$$
$$W_{c,s} := W_h \cap W_c^d,$$

we know that $\mathbf{u}_h \in U_c^d$ and $\boldsymbol{\sigma}_h \in W_{c,s} \subset W_c^d$. Note that for any $v \in U_c$ and $\boldsymbol{\alpha} \in W_c$, if we denote

$$b(\boldsymbol{\alpha}, v) := \int_\Omega \boldsymbol{\alpha} \cdot \nabla v \, dx - \sum_{e \in \mathcal{F}_p} \int_e (\boldsymbol{\alpha} \cdot \mathbf{n}_e)[v] \, ds,$$

$$b^*(v, \boldsymbol{\alpha}) := -\int_\Omega v \, \mathrm{div}\, \boldsymbol{\alpha} \, dx + \sum_{e \in \mathcal{F}_u^0} \int_e v[\boldsymbol{\alpha} \cdot \mathbf{n}] \, ds,$$

then for any $\mathbf{v} = (v_1, \ldots, v_d)^T \in U_c^d$ and $\boldsymbol{\alpha} = (\boldsymbol{\alpha}_1, \ldots, \boldsymbol{\alpha}_d)^T \in W_c^d$, we have

$$B(\boldsymbol{\alpha}, \mathbf{v}) = \sum_{k=1}^d b(\boldsymbol{\alpha}_k, v_k),$$

$$B^*(\mathbf{v}, \boldsymbol{\alpha}) = \sum_{k=1}^d b^*(v_k, \boldsymbol{\alpha}_k).$$

Some good properties of $b(\boldsymbol{\alpha}, v)$ and $b^*(v, \boldsymbol{\alpha})$ are proved in [16]. It is straight forward to extend these properties to B and B^*. Before we show these results, we first introduce several norms. In the space U_c^d, we define

$$\|\mathbf{v}\|_X^2 := \int_\Omega |\mathbf{v}|^2 \, dx + \sum_{e \in \mathcal{F}_u^0} h_e \int_\kappa |\mathbf{v}|^2 \, ds,$$

$$\|\mathbf{v}\|_Z^2 := \int_\Omega |\nabla \mathbf{v}|^2 \, dx + \sum_{e \in \mathcal{F}_p} h_e^{-1} \int_\kappa |[\mathbf{v}]|^2 \, ds.$$

Also, in the space W_c^d we define these norms:

$$\|\boldsymbol{\alpha}\|_{X'}^2 = \int_\Omega |\boldsymbol{\alpha}|^2 \, dx + \sum_{e \in \mathcal{F}_p} h_e \int_e |\boldsymbol{\alpha}\mathbf{n}|^2 \, ds,$$

$$\|\boldsymbol{\alpha}\|_{Z'}^2 = \int_\Omega |\nabla \cdot \boldsymbol{\alpha}|^2 \, dx + \sum_{e \in \mathcal{F}_u^0} h_e^{-1} \int_e |[\boldsymbol{\alpha}\mathbf{n}]|^2 \, ds.$$

In the following lemma, we show an inf–sup condition for $B^*(\mathbf{v}, \boldsymbol{\alpha})$. The proof is a generalization of the proof in [16].

Lemma 1. *There is a uniform constant $K > 0$ independent of h such that*

$$\inf_{\boldsymbol{\alpha} \in W_c^d} \sup_{\mathbf{v} \in U_c^d} \frac{B^*(\mathbf{v}, \boldsymbol{\alpha})}{\|\boldsymbol{\alpha}\|_{Z'} \|\mathbf{v}\|_X} \geq K.$$

Proof. It is sufficient to show that there are uniform constants $K > 0$ and $\tilde{K} > 0$ such that for any fixed $\boldsymbol{\alpha} \in W_c^d$ there is a nonzero $\mathbf{v} \in U_c^d$ such that

$$B^*(\mathbf{v}, \boldsymbol{\alpha}) \geq K\|\boldsymbol{\alpha}\|_{Z'}^2 \quad \text{and} \quad \|\mathbf{v}\|_X \leq \tilde{K}\|\boldsymbol{\alpha}\|_{Z'}.$$

Following the proof in [16], we know that for any fixed $\boldsymbol{\alpha}_k \in W_c$, $k = 1, \ldots, d$, there is a nonzero $v_{1,k} \in U_c$ with $v_{1,k}|_{\mathcal{F}_u^0} = 0$ such that

$$b^*(v_{1,k}, \boldsymbol{\alpha}_k) \geq K_1 \int_\Omega (\nabla \cdot \boldsymbol{\alpha}_k)^2 \, dx \quad \text{and} \quad \int_\Omega (v_{1,k})^2 \, dx \leq \int_\Omega (\nabla \cdot \boldsymbol{\alpha}_k)^2 \, dx.$$

Also, there is a nonzero $v_{2,k} \in U_c$ such that

$$b^*(v_{2,k}, \boldsymbol{\alpha}_k) = \sum_{e \in \mathcal{F}_u^0} h_e^{-1} \int_e [\boldsymbol{\alpha}_k \cdot \mathbf{n}]^2 \, ds \quad \text{and}$$

$$\int_\Omega (v_{2,k})^2 \, dx + \sum_{e \in \mathcal{F}_u^0} h_e \int_e |v_{2,k}|^2 \, ds \le K_2 \sum_{e \in \mathcal{F}_u^0} h_e^{-1} \int_e [\boldsymbol{\alpha}_k \cdot \mathbf{n}]^2 \, ds.$$

Define $\mathbf{v}_1 := (v_{1,1}, \ldots, v_{1,d})^T$ and $\mathbf{v}_2 := (v_{2,1}, \ldots, v_{2,d})^T$. Summing previous equations over k, we have

$$B^*(\mathbf{v}_1, \boldsymbol{\alpha}) \ge K_1 \int_\Omega |\nabla \cdot \boldsymbol{\alpha}|^2 \, dx \quad \text{and} \quad \int_\Omega |\mathbf{v}_1|^2 \, dx \le \int_\Omega |\nabla \cdot \boldsymbol{\alpha}|^2 \, dx,$$

$$B^*(\mathbf{v}_2, \boldsymbol{\alpha}) = \sum_{e \in \mathcal{F}_u^0} h_e^{-1} \int_e |[\boldsymbol{\alpha}\mathbf{n}]|^2 \, ds \quad \text{and}$$

$$\int_\Omega |\mathbf{v}_2|^2 \, dx + \sum_{e \in \mathcal{F}_u^0} h_e \int_e |\mathbf{v}_2|^2 \, ds \le K_2 \sum_{e \in \mathcal{F}_u^0} h_e^{-1} \int_e |[\boldsymbol{\alpha}\mathbf{n}]|^2 \, ds.$$

Take $\mathbf{v} = \mathbf{v}_1 + \mathbf{v}_2$. Since B^* is linear, we have

$$B^*(\mathbf{v}, \boldsymbol{\alpha}) = B^*(\mathbf{v}_1, \boldsymbol{\alpha}) + B^*(\mathbf{v}_2, \boldsymbol{\alpha}) \ge K \|\boldsymbol{\alpha}\|_{Z'}^2.$$

Also, we have

$$\|\mathbf{v}\|_X \le \|\mathbf{v}_1\|_X + \|\mathbf{v}_2\|_X \le \tilde{K} \|\boldsymbol{\alpha}\|_{Z'}. \quad \square$$

The inf–sup condition for $B^*(\mathbf{v}, \boldsymbol{\alpha})$ implies the existence of an operator $\mathcal{I} : H^1(\Omega)^d \to U_c^d$ such that

$$B^*(\mathcal{I}\mathbf{v} - \mathbf{v}, \boldsymbol{\alpha}) = 0, \qquad \forall \boldsymbol{\alpha} \in W_c^d, \tag{27}$$

Moreover, following proofs in [16], we have the stability and interpolation error estimate of the operator $\mathcal{I}$ as follows:

Lemma 2 (*Stability and Interpolation Error for $\mathcal{I}$*)**.** *For any* $\mathbf{u} \in H^1(\Omega)^d$, *we have*

$$\|\mathcal{I}\mathbf{u}\|_X + \|\mathcal{I}\mathbf{u}\|_Z \le K \|\mathbf{u}\|_{H^1(\Omega)^d}.$$

If $\mathbf{u} \in H^{k+1}(\Omega)^d$, *then*

$$\|\mathbf{u} - \mathcal{I}\mathbf{u}\| \le Kh^{k+1} |\mathbf{u}|_{H^{k+1}(\Omega)^d} \quad \text{and} \quad \|\mathbf{u} - \mathcal{I}\mathbf{u}\|_Z \le Kh^k |\mathbf{u}|_{H^{k+1}(\Omega)^d}.$$

Next, we will construct a special operator $\mathcal{J} : H(\mathbf{div}; \Omega)^d \to W_c^d$, which preserves the symmetry. Define

$$\Gamma_h := \left\{ \boldsymbol{\eta} : \boldsymbol{\eta} \Big|_\tau \in [P^k(\tau)]^{d \times d}, \boldsymbol{\eta} = -\boldsymbol{\eta}^T, \forall \tau \in \mathcal{T} \right\}.$$

Moreover, for any $(\boldsymbol{\alpha}, \mathbf{v}, \boldsymbol{\eta}) \in W_c^d \times U_c^d \times \Gamma_h$, we denote

$$\tilde{b}(\boldsymbol{\alpha}; \mathbf{v}, \boldsymbol{\eta}) := B(\boldsymbol{\alpha}, \mathbf{v}) - \int_\Omega \boldsymbol{\alpha} : \boldsymbol{\eta} \, dx,$$

and

$$\|(\mathbf{v}, \boldsymbol{\eta})\|_{\tilde{Z}}^2 := \int_\Omega |\boldsymbol{\eta} - \nabla \mathbf{v}|^2 dx + \sum_{e \in \mathcal{F}_p} h_e^{-1} \int |[\mathbf{v}]|^2 ds.$$

We will use the following lemma in [23]:

Lemma 3. *There is a uniform constant $K > 0$ independent of h such that*

$$\inf_{(\mathbf{v}, \boldsymbol{\eta}) \in U_c^d \times \Gamma_h} \sup_{\boldsymbol{\alpha} \in W_c^d} \frac{\tilde{b}(\boldsymbol{\alpha}; \mathbf{v}, \boldsymbol{\eta})}{\|\boldsymbol{\alpha}\|_{X'} \|(v, \boldsymbol{\eta})\|_{\tilde{Z}}} \ge K.$$

The inf–sup condition in Lemma 3 implies that for a given $\boldsymbol{\alpha} \in H(\mathbf{div}; \Omega)^d$, there is a unique solution $(\boldsymbol{\alpha}^*, \mathbf{v}^*, \boldsymbol{\eta}^*) \in W_c^d \times U_c^d \times \Gamma_h$ such that for any $(\boldsymbol{\beta}, \mathbf{v}, \boldsymbol{\eta}) \in W_c^d \times U_c^d \times \Gamma_h$,

$$\int_\Omega \boldsymbol{\alpha}^* : \boldsymbol{\beta} \, dx + \tilde{b}(\boldsymbol{\beta}; \mathbf{v}^*, \boldsymbol{\eta}^*) = \int_\Omega \boldsymbol{\alpha} : \boldsymbol{\beta} dx,$$

$$\tilde{b}(\boldsymbol{\alpha}^*; \mathbf{v}, \boldsymbol{\eta}) = \tilde{b}(\boldsymbol{\alpha}; \mathbf{v}, \boldsymbol{\eta}). \tag{28}$$

We define an operator $\mathcal{J} : H(\mathbf{div}; \Omega)^d \to W_c^d$ mapping $\boldsymbol{\alpha} \in H(\mathbf{div}; \Omega)^d$ to the solution $\boldsymbol{\alpha}^*$ of the above system and hence have

$$\tilde{b}(\mathcal{J}\boldsymbol{\alpha} - \boldsymbol{\alpha}; \mathbf{v}, \boldsymbol{\eta}) = 0, \qquad \forall(\mathbf{v}, \boldsymbol{\eta}) \in U_c^d \times \Gamma_h. \tag{29}$$

Lemma 4 (*Stability and interpolation error for* $\mathcal{J}$). *For any* $\boldsymbol{\alpha} \in H(\mathbf{div}; \Omega)^d$,

$$\|\mathcal{J}\boldsymbol{\alpha}\|_{X'} \le K \|\boldsymbol{\alpha}\|_{H(\mathbf{div}; \Omega)^d}, \tag{30}$$

and for any $\boldsymbol{\alpha} \in H^{k+1}(\Omega)^{d \times d}$,

$$\|\boldsymbol{\alpha} - \mathcal{J}\boldsymbol{\alpha}\| \le Kh^{k+1}|\boldsymbol{\alpha}|_{H^{k+1}(\Omega)^{d \times d}}. \tag{31}$$

Proof. Since $\mathcal{J}\boldsymbol{\alpha}$ is the solution of the problem (28), we have

$$\|\mathcal{J}\boldsymbol{\alpha}\|_{X'} \le K \|\boldsymbol{\alpha}\|_{X'} \le K \|\boldsymbol{\alpha}\|_{H(\mathbf{div}; \Omega)^d}. \tag{32}$$

On the other hand, from Eq. (28), for any $\tilde{\boldsymbol{\alpha}} \in W_c^d$ and $(\boldsymbol{\beta}, \mathbf{v}, \boldsymbol{\eta}) \in W_c^d \times U_c^d \times \Gamma_h$,

$$\int_\Omega (\mathcal{J}\boldsymbol{\alpha} - \tilde{\boldsymbol{\alpha}}) : \boldsymbol{\beta} \, dx + \tilde{b}(\boldsymbol{\beta}; \mathbf{v}^*, \boldsymbol{\eta}^*) = \int_\Omega (\boldsymbol{\alpha} - \tilde{\boldsymbol{\alpha}}) : \boldsymbol{\beta} dx,$$
$$\tilde{b}(\mathcal{J}\boldsymbol{\alpha} - \tilde{\boldsymbol{\alpha}}; \mathbf{v}, \boldsymbol{\eta}) = \tilde{b}(\boldsymbol{\alpha} - \tilde{\boldsymbol{\alpha}}; \mathbf{v}, \boldsymbol{\eta}). \tag{33}$$

By uniqueness of the solution of problem (28),

$$\left\|\mathcal{J}\boldsymbol{\alpha} - \tilde{\boldsymbol{\alpha}}\right\|_{X'} = \left\|\mathcal{J}(\boldsymbol{\alpha} - \tilde{\boldsymbol{\alpha}})\right\|_{X'} \le K \left\|\boldsymbol{\alpha} - \tilde{\boldsymbol{\alpha}}\right\|_{X'}. \tag{34}$$

Hence, we have

$$\|\mathcal{J}\boldsymbol{\alpha} - \boldsymbol{\alpha}\|_{X'} \le \left\|\mathcal{J}\boldsymbol{\alpha} - \tilde{\boldsymbol{\alpha}}\right\|_{X'} + \left\|\boldsymbol{\alpha} - \tilde{\boldsymbol{\alpha}}\right\|_{X'} \le K \left\|\boldsymbol{\alpha} - \tilde{\boldsymbol{\alpha}}\right\|_{X'}. \tag{35}$$

Taking $\tilde{\boldsymbol{\alpha}}$ as the (element-wise) standard conforming interpolant of $\boldsymbol{\alpha}$ yields the required bound. □

By the definition of the operator $\mathcal{J}$ and $\tilde{b}$, we can prove two important properties of $\mathcal{J}$ as in the following lemma.

Lemma 5. *For any* $\boldsymbol{\alpha} \in H(\mathbf{div}; \Omega)^d$, *we have*

$$B(\mathcal{J}\boldsymbol{\alpha} - \boldsymbol{\alpha}, \mathbf{v}) = 0, \qquad \forall \mathbf{v} \in U_c^d.$$

Moreover, if $\boldsymbol{\alpha}^T = \boldsymbol{\alpha}$, *then* $\mathcal{J}\boldsymbol{\alpha} = (\mathcal{J}\boldsymbol{\alpha})^T$.

Proof. By taking $\boldsymbol{\eta} = \mathbf{0}$ in Eq. (29), we immediately get

$$B(\mathcal{J}\boldsymbol{\alpha} - \boldsymbol{\alpha}; \mathbf{v}) = \tilde{b}(\mathcal{J}\boldsymbol{\alpha} - \boldsymbol{\alpha}; \mathbf{v}, \mathbf{0}) = 0, \qquad \forall \mathbf{v} \in U_c^d.$$

On the other hand, if we take $\mathbf{v} = \mathbf{0}$ in Eq. (29), we obtain

$$\int_\Omega (\mathcal{J}\boldsymbol{\alpha} - \boldsymbol{\alpha}) : \boldsymbol{\eta} \, dx = -\tilde{b}(\mathcal{J}\boldsymbol{\alpha} - \boldsymbol{\alpha}, \mathbf{0}, \boldsymbol{\eta}) = 0. \qquad \forall \boldsymbol{\eta} \in \Gamma_h.$$

Since $\boldsymbol{\alpha}$ is symmetric and $\boldsymbol{\eta}$ is skew symmetric, we have

$$\int_\Omega \mathcal{J}\boldsymbol{\alpha} : \boldsymbol{\eta} \, dx = \int_\Omega \boldsymbol{\alpha} : \boldsymbol{\eta} \, dx = 0, \qquad \forall \boldsymbol{\eta} \in \Gamma_h.$$

Hence, we conclude that $\mathcal{J}\boldsymbol{\alpha}$ is symmetric too. □

Now we are ready to show the main result of our paper that our scheme is L^2 stable and can obtain the optimal convergence rate such that the constant in the convergence estimate is independent of the Lamé's first parameter λ. Also, the wave energy is conserved.

To begin with, we define some norms. We define $\|\cdot\|_\rho$ and $\|\cdot\|_\mathbf{A}$ by

$$\|\mathbf{v}\|_\rho^2 := \int_\Omega \rho \mathbf{v} \cdot \mathbf{v} dx \quad \text{and} \quad \|\boldsymbol{\alpha}\|_\mathbf{A}^2 := \int_\Omega \mathbf{A}\boldsymbol{\alpha} : \boldsymbol{\alpha} dx$$

and the energy norm $\|\cdot\|_E$ by

$$\|\mathbf{v}, \boldsymbol{\alpha}\|_E^2 := \|\mathbf{v}\|_\rho^2 + \|\boldsymbol{\alpha}\|_\mathbf{A}^2.$$

Theorem 6. *Let* $\mathbf{u} \in W^{1,1}(0, T; H^{k+1}(\Omega)^d)$, $\boldsymbol{\sigma} \in W^{1,1}(0, T; H^{k+1}(\Omega)^{d\times d})$ *be the solution of* (2) *and* (3)*, and* $\mathbf{u}_h \in U_c^d$, $\boldsymbol{\sigma}_h \in W_{c,s}$ *be the solutions of* (15)–(18)*, then we have the following stability estimate*

$$\|\mathbf{u}_h, \boldsymbol{\sigma}_h\|_E \leq K \left\{ \|\mathbf{u}_h(0, \cdot), \boldsymbol{\sigma}_h(0, \cdot)\|_E + \int_0^T |\mathbf{f}| \, ds \right\} \tag{36}$$

and the following conversation of energy relation:

$$\frac{1}{2} \frac{\partial}{\partial t} \left\{ \int_{\Omega''} \rho |\mathbf{u}_h|^2 \, dx + \int_{\Omega'} \mathbf{A} \boldsymbol{\sigma}_h : \boldsymbol{\sigma}_h \, dx \right\} = \int_{\partial \Omega'} \mathbf{u}_h \cdot \boldsymbol{\sigma}_h \mathbf{n} \, dx + \int_{\Omega'} \mathbf{f} \cdot \mathbf{u}_h \, dx, \tag{37}$$

where Ω' *is a subdomain formed by union of* $\mathcal{S}(\nu)$, $\nu \in \mathcal{N}_1 \subset \mathcal{N}$ *and* Ω'' *is defined by the union of all* $\mathcal{R}(\kappa)$, $\kappa \in \mathcal{F}_u$ *that have nonempty intersection with* Ω'*. Also, the following convergence estimate holds:*

$$\|\mathbf{u} - \mathbf{u}_h, \boldsymbol{\sigma} - \boldsymbol{\sigma}_h\|_E \leq \|(\mathcal{I}\mathbf{u} - \mathbf{u}_h)(0, \cdot), (\mathcal{J}\boldsymbol{\sigma} - \boldsymbol{\sigma}_h)(0, \cdot)\|_E$$
$$+ Kh^{k+1} \left(\|\mathbf{u}\|_{W^{1,1}(0,T;H^{k+1}(\Omega)^d)} + \|\boldsymbol{\sigma}\|_{W^{1,1}(0,T;H^{k+1}(\Omega)^{d\times d})} \right), \tag{38}$$

where the constant K is independent of the Lamé's first parameter λ.

Proof. Note that from continuity conditions (9) and (10), we know that $\mathbf{u}_h \in U_c^d$ and $\boldsymbol{\sigma}_h \in W_{c,s}$. Also, it is easy to show that for any $\mathbf{v} \in U_c^d$, $\boldsymbol{\alpha} \in W_c^d$, $\widehat{\mathbf{v}} \in \widehat{U}_h^d$, and $\widehat{\boldsymbol{\alpha}} \in \widehat{W}_h^d$, we have

$$D^*(\widehat{\boldsymbol{\alpha}}, \mathbf{v}) = 0,$$
$$D(\widehat{\mathbf{v}}, \boldsymbol{\alpha}) = 0.$$

Therefore, if we choose test functions $\mathbf{v}_h$ and $\boldsymbol{\alpha}_h$ in spaces U_c^d and $W_{c,s}$, respectively, then the solutions of the SDG scheme (15)–(18) satisfy the followings:

$$\int_{\Omega} \rho \frac{\partial \mathbf{u}_h}{dt} \cdot \mathbf{v}_h \, dx + B(\boldsymbol{\sigma}_h, \mathbf{v}_h) = \int_{\Omega} \mathbf{f} \cdot \mathbf{v}_h \, dx, \tag{39}$$

$$\int_{\Omega} \mathbf{A} \frac{\partial \boldsymbol{\sigma}_h}{dt} : \boldsymbol{\alpha}_h \, dx - B^*(\mathbf{u}_h, \boldsymbol{\alpha}_h) = 0. \tag{40}$$

By integration by parts, we also know that

$$B(\boldsymbol{\alpha}, \mathbf{v}) = B^*(\mathbf{v}, \boldsymbol{\alpha}), \qquad \forall \mathbf{v} \in U_c^d, \qquad \forall \boldsymbol{\alpha} \in W_c^d. \tag{41}$$

We take $\mathbf{v}_h = \mathbf{u}_h$ and $\boldsymbol{\alpha}_h = \boldsymbol{\sigma}_h$. Adding (39) and (40) and by using the Cauchy–Schwarz inequality, we obtain

$$\frac{1}{2} \frac{d}{dt} \left\{ \|\mathbf{u}_h\|_\rho^2 + \|\boldsymbol{\sigma}_h\|_\mathbf{A}^2 \right\} = \int_{\Omega} \mathbf{f} \cdot \mathbf{u}_h \, dx \leq \rho^{-\frac{1}{2}} \|\mathbf{f}\| \|\mathbf{u}_h\|_\rho.$$

Integrate in time from 0 to t, we have

$$\|\mathbf{u}_h, \boldsymbol{\sigma}_h\|_E^2 \leq \|\mathbf{u}_h(0, \cdot), \boldsymbol{\sigma}_h(0, \cdot)\|_E^2 + 2\rho^{-\frac{1}{2}} \max_{0 \leq t \leq T} \|\mathbf{u}_h\|_\rho \int_0^t \|\mathbf{f}\| \, ds$$

$$\leq \|\mathbf{u}_h(0, \cdot), \boldsymbol{\sigma}_h(0, \cdot)\|_E^2 + \frac{1}{2} \max_{0 \leq t \leq T} \|\mathbf{u}_h\|_\rho^2 + 2\rho^{-1} \left\{ \int_0^T \|\mathbf{f}\| \, ds \right\}^2. \tag{42}$$

Hence the stability estimate (36) follows. The conservation of energy (37) following from adding (39) and (40), and putting $\mathbf{v}_h = \mathbf{u}_h \chi_{\Omega''}$, $\boldsymbol{\alpha}_h = \boldsymbol{\sigma}_h \chi_{\Omega'}$.

To show the convergence estimate (38), we take $\mathbf{v} = \mathbf{v}_h$ and $\boldsymbol{\alpha} = \boldsymbol{\alpha}_h$ in (11) and (12), and then subtract them by Eqs. (39) and (40), respectively, and get

$$\int_{\Omega} \rho \frac{\partial}{\partial t}(\mathbf{u} - \mathbf{u}_h) \cdot \mathbf{v}_h \, dx + B(\boldsymbol{\sigma} - \boldsymbol{\sigma}_h, \mathbf{v_h}) = 0, \qquad \forall \mathbf{v_h} \in U_c^d, \tag{43}$$

$$\int_{\Omega} \mathbf{A} \frac{\partial}{\partial t}(\boldsymbol{\sigma} - \boldsymbol{\sigma}_h) : \boldsymbol{\alpha}_h \, dx - B^*(\mathbf{u} - \mathbf{u}_h, \boldsymbol{\alpha}_h) = 0, \qquad \forall \boldsymbol{\alpha}_h \in W_{c,s}. \tag{44}$$

Using the properties of $\mathcal{I}$ and $\mathcal{J}$ from (27) and Lemma 5, we have

$$\int_{\Omega} \rho \frac{\partial}{\partial t}(\mathbf{u} - \mathbf{u}_h) \cdot \mathbf{v}_h \, dx + B(\mathcal{J}\boldsymbol{\sigma} - \boldsymbol{\sigma}_h, \mathbf{v_h}) = 0, \qquad \forall \mathbf{v_h} \in U_c^d, \tag{45}$$

$$\int_{\Omega} \mathbf{A} \frac{\partial}{\partial t}(\boldsymbol{\sigma} - \boldsymbol{\sigma}_h) : \boldsymbol{\alpha}_h \, dx - B^*(\mathcal{I}\mathbf{u} - \mathbf{u}_h, \boldsymbol{\alpha}_h) = 0, \qquad \forall \boldsymbol{\alpha}_h \in W_{c,s}. \tag{46}$$

Since the exact solution σ is symmetric, Lemma 5 implies that $\mathcal{J}\sigma$ is also symmetric. We take $\mathbf{v}_h = \mathcal{I}\mathbf{u} - \mathbf{u}_h$ and $\alpha_h = \mathcal{J}\sigma - \sigma_h$. Summing the above two equations and by using (41), we have

$$\int_\Omega \rho \frac{\partial}{\partial t}(\mathcal{I}\mathbf{u} - \mathbf{u}_h) \cdot (\mathcal{I}\mathbf{u} - \mathbf{u}_h)\, dx + \int_\Omega \mathbf{A}\frac{\partial}{\partial t}(\mathcal{J}\sigma - \sigma_h) : (\mathcal{J}\sigma - \sigma_h)\, dx$$
$$= \int_\Omega \rho \frac{\partial}{\partial t}(\mathcal{I}\mathbf{u} - \mathbf{u}) \cdot (\mathcal{I}\mathbf{u} - \mathbf{u}_h)\, dx + \int_\Omega \mathbf{A}\frac{\partial}{\partial t}(\mathcal{J}\sigma - \sigma) : (\mathcal{J}\sigma - \sigma_h)\, dx. \tag{47}$$

Equivalently,

$$\frac{1}{2}e_t = \int_\Omega \rho \frac{\partial}{\partial t}(\mathcal{I}\mathbf{u} - \mathbf{u}) \cdot (\mathcal{I}\mathbf{u} - \mathbf{u}_h)\, dx + \int_\Omega \mathbf{A}\frac{\partial}{\partial t}(\mathcal{J}\sigma - \sigma) : (\mathcal{J}\sigma - \sigma_h)\, dx, \tag{48}$$

where $e(t) := \|\mathcal{I}\mathbf{u} - \mathbf{u}_h(\cdot, t), \mathcal{J}\sigma - \sigma_h(\cdot, t)\|_E^2$. Hence, we have

$$\frac{1}{2}e_t \le \left\| \frac{\partial}{\partial t}(\mathcal{I}\mathbf{u} - \mathbf{u}) \right\|_\rho \|\mathcal{I}\mathbf{u} - \mathbf{u}_h\|_\rho + \left\| \frac{\partial}{\partial t}(\mathcal{J}\sigma - \sigma) \right\|_\mathbf{A} \|\mathcal{J}\sigma - \sigma_h\|_\mathbf{A}.$$

Using the interpolation error estimates in Lemma 2 and Lemma 4 and the fact that the operators $\mathcal{I}$ and $\mathcal{J}$ commute with the time derivative, we have

$$e_t \le Kh^{k+1} \left\{ |\mathbf{u}_t|_{H^{k+1}(\Omega)^d} \|\mathcal{I}\mathbf{u} - \mathbf{u}_h\|_\rho + |\sigma_t|_{H^{k+1}(\Omega)^{d\times d}} \|\mathcal{J}\sigma - \sigma_h\|_\mathbf{A} \right\}. \tag{49}$$

Then we integrate this equation with respect to time from 0 to t. Note that

$$Kh^{k+1} \int_0^t |\mathbf{u}_t|_{H^{k+1}(\Omega)^d} \|\mathcal{I}\mathbf{u} - \mathbf{u}_h\|_\rho\, ds$$
$$\le Kh^{2k+2} \left(\int_0^t |\mathbf{u}_t|_{H^{k+1}(\Omega)^d}\, ds \right)^2 + \frac{1}{2} \max_{0 \le s \le t} \|\mathcal{I}\mathbf{u}(\cdot, s) - \mathbf{u}_h(\cdot, s)\|_\rho^2, \tag{50}$$

and a similar relation holds for σ. Therefore we have

$$e(t) \le e(0) + Kh^{2k+2} \left\{ \left(\int_0^t |\mathbf{u}_t|_{H^{k+1}(\Omega)^d}\, ds \right)^2 + \left(\int_0^t |\sigma_t|_{H^{k+1}(\Omega)^{d\times d}}\, ds \right)^2 \right\}. \tag{51}$$

Hence for any $0 \le t \le T$, we have

$$\|\mathcal{I}\mathbf{u} - \mathbf{u}_h, \mathcal{J}\sigma - \sigma_h\|_E \le \|(\mathcal{I}\mathbf{u} - \mathbf{u}_h)(0, \cdot), (\mathcal{J}\sigma - \sigma_h)(0, \cdot)\|_E$$
$$+ Kh^{k+1} \int_0^t |\mathbf{u}_t|_{H^{k+1}(\Omega)^d} + |\sigma_t|_{H^{k+1}(\Omega)^{d\times d}}\, ds. \tag{52}$$

Using the interpolation error estimates in Lemma 2 and Lemma 4, and the Sobolev inequality $\max_{0 \le t \le T} |v(t)| \le K\|v\|_{W^{1,1}(0,T)}$ the convergence estimate follows. The constant in (49) is independent of λ, since

$$\|\cdot\|_\mathbf{A} \le \frac{1}{2\mu} \|\cdot\|. \quad \square$$

Remark 1. In the above theorem, $\mathcal{N}_1$ is a subset of the set $\mathcal{N}$. Thus, the Ω' is a subdomain of Ω, and Ω'' is obtained from Ω'. In this case, (37) gives a local energy conservation identity. In addition, if we take $\mathcal{N}_1 = \mathcal{N}$, then $\Omega' = \Omega'' = \Omega$. In this case, (37) gives a global energy conservation identity.

Remark 2. An SDG method with proofs of the well-posedness and error estimate was proposed for the static linear elastic equation in [23], in which the symmetry of the stress tensor is imposed weakly via Lagrange multipliers. Our staggered hybrid method can also be applied to the static elastic equation. The proofs for the time-dependent case in this paper can be modified easily in order to prove the well-posedness and optimal error estimate for the static case as in [23].

5. Analysis for fully discrete solutions

In this section, we will analyze the fully discrete scheme (19)–(22). We will show a sufficient condition on the time step Δt for the stability of the discrete scheme. Also, we will discuss the convergence of this scheme. In the following theorem, we present a stability condition. For this purpose, we can assume that $\mathbf{f} = 0$ to simplify the analysis.

Theorem 7. *For simplicity, we take* $\mathbf{f} = 0$. *Define*

$$K_C := \frac{1}{2} \sup_{\mathbf{v}_h \in U_h^d, \, \alpha_h \in W_h} \frac{B(\alpha_h, \mathbf{v}_h)}{\|\mathbf{v}_h\|_\rho \|\alpha_h\|_\mathbf{A}}.$$

If the time step Δt *satisfies* $\Delta t < K_C^{-1}$, *then the fully discrete scheme* (19)–(22) *is stable.*

Proof. Substitute $\mathbf{v}_h = \mathbf{u}_h^{n+1} + \mathbf{u}_h^n, \boldsymbol{\alpha}_h = \boldsymbol{\sigma}_h^{n+\frac{3}{2}} + \boldsymbol{\sigma}_h^{n+\frac{1}{2}}$ into Eqs. (19) and (20) respectively,

$$\int_\Omega \rho \delta_t \mathbf{u}_h^{n+\frac{1}{2}} \cdot \left(\mathbf{u}_h^{n+1} + \mathbf{u}_h^n\right) dx + B\left(\boldsymbol{\sigma}_h^{n+\frac{1}{2}}, \mathbf{u}_h^{n+1} + \mathbf{u}_h^n\right) = \int_\Omega \mathbf{f}^{n+\frac{1}{2}} \cdot \left(\mathbf{u}_h^{n+1} + \mathbf{u}_h^n\right), \tag{53}$$

$$\int_\Omega \mathbf{A}\delta_t \boldsymbol{\sigma}_h^{n+1} : \left(\boldsymbol{\sigma}_h^{n+\frac{3}{2}} + \boldsymbol{\sigma}_h^{n+\frac{1}{2}}\right) - B^*\left(\mathbf{u}_h^{n+1}, \boldsymbol{\sigma}_h^{n+\frac{3}{2}} + \boldsymbol{\sigma}_h^{n+\frac{1}{2}}\right) = 0, \tag{54}$$

where we have used

$$D^*\left(\widehat{\boldsymbol{\sigma}}_h^{n+1} + \widehat{\boldsymbol{\sigma}}_h^n, \mathbf{u}_h^{n+1} + \mathbf{u}_h^n\right) = D\left(\widehat{\mathbf{u}}_h^{n+\frac{3}{2}} + \widehat{\mathbf{u}}_h^{n+\frac{1}{2}}, \boldsymbol{\sigma}_h^{n+\frac{3}{2}} + \boldsymbol{\sigma}_h^{n+\frac{1}{2}}\right) = 0 \tag{55}$$

from (21) and (22). Fix an integer $N > 0$. Summing equation (53) and (54) from 0 to $N - 1$, we have

$$\left\|\mathbf{u}_h^N, \boldsymbol{\sigma}_h^{N+\frac{1}{2}}\right\|_E^2 = \left\|\mathbf{u}_h^0, \boldsymbol{\sigma}_h^{\frac{1}{2}}\right\|_E^2 + \Delta t \, B^*\left(\mathbf{u}_h^N, \boldsymbol{\sigma}_h^{N+\frac{1}{2}}\right) - \Delta t \, B\left(\boldsymbol{\sigma}_h^{\frac{1}{2}}, \mathbf{u}_h^0\right), \tag{56}$$

since we have

$$B(\boldsymbol{\sigma}_h^{n+\frac{1}{2}}, \mathbf{u}_h^{n+1}) = B^*(\mathbf{u}_h^{n+1}, \boldsymbol{\sigma}_h^{n+\frac{1}{2}}) \tag{57}$$

from (41). Using the Cauchy–Schwarz inequality, we have

$$\left| B\left(\boldsymbol{\sigma}_h^{\frac{1}{2}}, \mathbf{u}_h^0\right) \right| \le 2K_C \left\|\mathbf{u}_h^0\right\|_\rho \left\|\boldsymbol{\sigma}_h^{\frac{1}{2}}\right\|_A \le K_C \left\|\mathbf{u}_h^0, \boldsymbol{\sigma}_h^{\frac{1}{2}}\right\|_E^2. \tag{58}$$

Similarly,

$$\left| B^*\left(\mathbf{u}_h^N, \boldsymbol{\sigma}_h^{N+\frac{1}{2}}\right) \right| \le K_C \left\|\mathbf{u}_h^N, \boldsymbol{\sigma}_h^{N+\frac{1}{2}}\right\|_E^2. \tag{59}$$

From (56)–(59), we have

$$\left\|\mathbf{u}_h^N, \boldsymbol{\sigma}_h^{N+\frac{1}{2}}\right\|_E^2 \le \frac{1 + \Delta t \, K_C}{1 - \Delta t \, K_C} \left\|\mathbf{u}_h^0, \boldsymbol{\sigma}_h^{\frac{1}{2}}\right\|_E^2, \tag{60}$$

provided that $\Delta t < K_C^{-1}$. $\square$

We note that the number K_C satisfies

$$K_C \le \widetilde{K}_C := \frac{1}{2}\left\|\mathbf{M}_u^{-\frac{1}{2}}\mathbf{B}_h\mathbf{M}_\sigma^{-\frac{1}{2}}\right\|_2.$$

Hence we can determine a sufficiently small time step before the simulation.

Next, we will discuss the convergence of the fully discrete scheme (19)–(22). We would like to bound the errors given by

$$\mathbf{E}_u^n := \mathbf{u}_h^n - \mathbf{u}^n \quad \text{and} \quad \mathbf{E}_\sigma^{n+\frac{1}{2}} := \boldsymbol{\sigma}_h^{n+\frac{1}{2}} - \boldsymbol{\sigma}^{n+\frac{1}{2}}.$$

We rewrite these errors by

$$\mathbf{E}_u^n = (\mathbf{u}_h^n - \mathcal{I}\mathbf{u}^n) + (\mathcal{I}\mathbf{u}^n - \mathbf{u}^n) =: \mathbf{e}_u^n + (\mathcal{I}\mathbf{u}^n - \mathbf{u}^n),$$

$$\mathbf{E}_\sigma^{n+\frac{1}{2}} = (\boldsymbol{\sigma}_h^{n+\frac{1}{2}} - \mathcal{J}\boldsymbol{\sigma}^{n+\frac{1}{2}}) + (\mathcal{J}\boldsymbol{\sigma}^{n+\frac{1}{2}} - \boldsymbol{\sigma}^{n+\frac{1}{2}}) := \mathbf{e}_\sigma^{n+\frac{1}{2}} + (\mathcal{J}\boldsymbol{\sigma}^{n+\frac{1}{2}} - \boldsymbol{\sigma}^{n+\frac{1}{2}}).$$

The following theorem shows the convergence of the fully discrete scheme. Note that in Lemmas 2 and 4, we have already provided an error estimates of order $\mathcal{O}(h^{k+1})$ for the interpolation operators $\mathcal{I}$ and $\mathcal{J}$. Therefore, it suffices to bound $\mathbf{e}_u^n$ and $\mathbf{e}_\sigma^{n+\frac{1}{2}}$ with order $\mathcal{O}(\Delta t^2 + h^{k+1})$.

Theorem 8. *Let* $\mathbf{u} \in W^{1,1}\left(0, T; H^{k+1}(\Omega)^d\right) \cap W^{2,\infty}\left(0, T; L^2(\Omega)^d\right)$ *and* $\boldsymbol{\sigma} \in W^{1,1}\left(0, T; H^{k+1}(\Omega)^{d \times d}\right) \cap W^{2,\infty}\left(0, T; L^2(\Omega)^{d \times d}\right)$ *be the solutions of* (2) *and* (3)*, and* $\mathbf{u}_h^n \in U_c^d, \boldsymbol{\sigma}_h^{n+\frac{1}{2}} \in W_c^d$ *be the solution of the fully discrete scheme* (19)–(22)*, then the following error estimates hold:*

$$\left\|\mathbf{E}_u^n, \mathbf{E}_\sigma^{n+\frac{1}{2}}\right\|_E \le \left\|\mathbf{E}_u^0, \mathbf{E}_\sigma^{\frac{1}{2}}\right\|_E + K(\Delta t^2 + h^{k+1})\Big(\|\mathbf{u}\|_{W^{1,1}(0,T;H^{k+1}(\Omega)^d)} + |\mathbf{u}|_{W^{2,\infty}(0,T;L^2(\Omega)^d)}$$

$$+ \|\boldsymbol{\sigma}\|_{W^{1,1}(0,T;H^{k+1}(\Omega)^{d \times d})} + |\boldsymbol{\sigma}|_{W^{2,\infty}(0,T;L^2(\Omega)^{d \times d})}\Big), \tag{61}$$

for any $n\Delta t \le T$.

Proof. Taking t and the test functions $\mathbf{v}$ and $\boldsymbol{\alpha}$ accordingly in (11) and (12), and summing over all the simplex τ, for any $\mathbf{v}_h \in U_h^d$ and $\boldsymbol{\alpha}_h \in W_h$, we have

$$\int_\Omega \rho \frac{\partial \mathbf{u}^{n+\frac{1}{2}}}{\partial t} \cdot \mathbf{v}_h + B(\boldsymbol{\sigma}^{n+\frac{1}{2}}, \mathbf{v}_h) = \int_\Omega \mathbf{f}^{n+\frac{1}{2}} \cdot \mathbf{v}_h, \tag{62}$$

$$\int_\Omega A \frac{\partial \boldsymbol{\sigma}^{n+1}}{\partial t} : \boldsymbol{\alpha}_h - B^*(\mathbf{u}^{n+1}, \boldsymbol{\alpha}_h) = 0. \tag{63}$$

According to (19) and (20),

$$\int_\Omega \rho \delta_t \mathbf{u}_h^{n+\frac{1}{2}} \cdot \mathbf{v}_h dx + B(\boldsymbol{\sigma}_h^{n+\frac{1}{2}}, \mathbf{v}_h) - \frac{1}{2} D^* \left(\widehat{\boldsymbol{\sigma}}_h^{n+1} + \widehat{\boldsymbol{\sigma}}_h^{n}, \mathbf{v}_h \right) = \int_\Omega \mathbf{f}^{n+\frac{1}{2}} \cdot \mathbf{v}_h dx, \tag{64}$$

$$\int_\Omega A \delta_t \boldsymbol{\sigma}_h^{n+1} : \boldsymbol{\alpha}_h dx - B^*(\mathbf{u}_h^{n+1}, \boldsymbol{\alpha}_h) + \frac{1}{2} D \left(\widehat{\mathbf{u}}_h^{n+\frac{3}{2}} + \widehat{\mathbf{u}}_h^{n+\frac{1}{2}}, \boldsymbol{\alpha}_h \right) = 0. \tag{65}$$

Apply the definition of $\mathbf{e}_u$ to (64),

$$\int_\Omega \rho \delta_t \mathbf{e}_u^{n+\frac{1}{2}} \mathbf{v}_h + B(\mathbf{e}_\sigma^{n+\frac{1}{2}}, \mathbf{v}_h) - \frac{1}{2} D^* \left(\widehat{\boldsymbol{\sigma}}_h^{n+1} + \widehat{\boldsymbol{\sigma}}_h^{n}, \mathbf{v}_h \right)$$
$$= \int_\Omega \mathbf{f}^{n+\frac{1}{2}} \cdot \mathbf{v}_h - \int_\Omega \rho \delta_t \mathcal{I} \mathbf{u}^{n+\frac{1}{2}} \mathbf{v}_h - B(\mathcal{J} \boldsymbol{\sigma}^{n+\frac{1}{2}}, \mathbf{v}_h). \tag{66}$$

Similarly, we can rewrite (65) as

$$\int_\Omega A \delta_t \mathbf{e}_\sigma^{n+1} : \boldsymbol{\alpha}_h - B^*(\mathbf{e}_u^{n+1}, \boldsymbol{\alpha}_h) + \frac{1}{2} D \left(\widehat{\mathbf{u}}_h^{n+\frac{3}{2}} + \widehat{\mathbf{u}}_h^{n+\frac{1}{2}}, \boldsymbol{\alpha}_h \right)$$
$$= - \int_\Omega A \delta_t \mathcal{J} \boldsymbol{\sigma}^{n+1} : \boldsymbol{\alpha}_h + B^*(\mathcal{I} \mathbf{u}^{n+1}, \boldsymbol{\alpha}_h). \tag{67}$$

By the definition of $\mathcal{I}$ and $\mathcal{J}$,

$$B(\boldsymbol{\sigma}^{n+\frac{1}{2}} - \mathcal{J} \boldsymbol{\sigma}^{n+\frac{1}{2}}, \mathbf{v}_h) = B^*(\mathbf{u}^{n+1} - \mathcal{I} \mathbf{u}^{n+1}, \boldsymbol{\alpha}_h) = 0. \tag{68}$$

Subtract (62) from (66) and using (68),

$$\int_\Omega \rho \delta_t \mathbf{e}_u^{n+\frac{1}{2}} \cdot \mathbf{v}_h + B(\mathbf{e}_\sigma^{n+\frac{1}{2}}, \mathbf{v}_h) - \frac{1}{2} D^* \left(\widehat{\boldsymbol{\sigma}}_h^{n+1} + \widehat{\boldsymbol{\sigma}}_h^{n}, \mathbf{v}_h \right) = \int_\Omega \rho \left(\frac{\partial \mathbf{u}^{n+\frac{1}{2}}}{\partial t} - \delta_t \mathcal{I} \mathbf{u}^{n+\frac{1}{2}} \right) \mathbf{v}_h. \tag{69}$$

Subtract (63) from (67) and using (68),

$$\int_\Omega A \delta_t \mathbf{e}_\sigma^{n+1} : \boldsymbol{\alpha}_h - B^*(\mathbf{e}_u^{n+1}, \boldsymbol{\alpha}_h) + \frac{1}{2} D \left(\widehat{\mathbf{u}}_h^{n+\frac{3}{2}} + \widehat{\mathbf{u}}_h^{n+\frac{1}{2}}, \boldsymbol{\alpha}_h \right)$$
$$= \int_\Omega A \left(\frac{\partial \boldsymbol{\sigma}^{n+1}}{\partial t} - \delta_t \mathcal{J} \boldsymbol{\sigma}^{n+1} \right) : \boldsymbol{\alpha}_h. \tag{70}$$

We note that from (21) and (22),

$$D^* \left(\widehat{\boldsymbol{\sigma}}_h^{n+1} + \widehat{\boldsymbol{\sigma}}_h^{n}, \mathbf{e}_u^{n+1} + \mathbf{e}_u^{n} \right) = D \left(\widehat{\mathbf{u}}_h^{n+\frac{3}{2}} + \widehat{\mathbf{u}}_h^{n+\frac{1}{2}}, \mathbf{e}_\sigma^{n+\frac{3}{2}} + \mathbf{e}_\sigma^{n+\frac{1}{2}} \right) = 0. \tag{71}$$

Also, by (41),

$$B(\mathbf{e}_\sigma^{n+\frac{1}{2}}, \mathbf{e}_u^{n+1}) = B^*(\mathbf{e}_u^{n+1}, \mathbf{e}_\sigma^{n+\frac{1}{2}}). \tag{72}$$

Sum (69) and (70), substitute $\mathbf{v}_h = \mathbf{e}_u^{n+1} + \mathbf{e}_u^{n}$, $\boldsymbol{\alpha}_h = \mathbf{e}_\sigma^{n+\frac{3}{2}} + \mathbf{e}_\sigma^{n+\frac{1}{2}}$, and use (71) and (72), we have

$$\int_\Omega \rho \delta_t \mathbf{e}_u^{n+\frac{1}{2}} (\mathbf{e}_u^{n+1} + \mathbf{e}_u^{n}) + \int_\Omega A \delta_t \mathbf{e}_\sigma^{n+1} : (\mathbf{e}_\sigma^{n+\frac{3}{2}} + \mathbf{e}_\sigma^{n+\frac{1}{2}}) + B(\mathbf{e}_\sigma^{n+\frac{1}{2}}, \mathbf{e}_u^{n}) - B^*(\mathbf{e}_u^{n+1}, \mathbf{e}_\sigma^{n+\frac{3}{2}})$$
$$= \int_\Omega \rho \left(\frac{\partial \mathbf{u}^{n+\frac{1}{2}}}{\partial t} - \delta_t \mathcal{I} \mathbf{u}^{n+\frac{1}{2}} \right) \cdot (\mathbf{e}_u^{n+1} + \mathbf{e}_u^{n}) + \int_\Omega A \left(\frac{\partial \boldsymbol{\sigma}^{n+1}}{\partial t} - \delta_t \mathcal{J} \boldsymbol{\sigma}^{n+1} \right) : (\mathbf{e}_\sigma^{n+\frac{3}{2}} + \mathbf{e}_\sigma^{n+\frac{1}{2}}). \tag{73}$$

Simplify left hand side and apply Cauchy–Schwarz inequality to the right hand side, we have

$$\frac{1}{\Delta t}\left(\left\|\mathbf{e}_u^{n+1}, \mathbf{e}_\sigma^{n+\frac{3}{2}}\right\|_E^2 - \left\|\mathbf{e}_u^n, \mathbf{e}_\sigma^{n+\frac{1}{2}}\right\|_E^2\right) + B(\mathbf{e}_\sigma^{n+\frac{1}{2}}, \mathbf{e}_u^n) - B^*(\mathbf{e}_u^{n+1}, \mathbf{e}_\sigma^{n+\frac{3}{2}})$$
$$\leq \left\|\frac{\partial \mathbf{u}^{n+\frac{1}{2}}}{\partial t} - \delta_t \mathcal{I} \mathbf{u}^{n+\frac{1}{2}}\right\|_\rho \left\|\mathbf{e}_u^{n+1} + \mathbf{e}_u^n\right\|_\rho + \left\|\frac{\partial \boldsymbol{\sigma}^{n+1}}{\partial t} - \delta_t \mathcal{J} \boldsymbol{\sigma}^{n+1}\right\|_A \left\|\mathbf{e}_\sigma^{n+\frac{3}{2}} + \mathbf{e}_\sigma^{n+\frac{1}{2}}\right\|_A. \tag{74}$$

We note that

$$\left|B(\mathbf{e}_\sigma^{n+\frac{1}{2}}, \mathbf{e}_u^n)\right| \leq \frac{1}{2}K_C\left\|\mathbf{e}_u^n, \mathbf{e}_\sigma^{n+\frac{1}{2}}\right\|_E^2, \tag{75}$$

$$\left|B^*(\mathbf{e}_u^{n+1}, \mathbf{e}_\sigma^{n+\frac{3}{2}})\right| \leq \frac{1}{2}K_C p\left\|\mathbf{e}_u^{n+1}, \mathbf{e}_\sigma^{n+\frac{3}{2}}\right\|_E^2. \tag{76}$$

From (74)–(76) and Cauchy–Schwarz inequality,

$$\left\|\mathbf{e}_u^{n+1}, \mathbf{e}_\sigma^{n+\frac{3}{2}}\right\|_E^2 - \left\|\mathbf{e}_u^n, \mathbf{e}_\sigma^{n+\frac{1}{2}}\right\|_E^2 \leq K\Delta t\left(\left\|\mathbf{e}_u^{n+1}, \mathbf{e}_\sigma^{n+\frac{3}{2}}\right\|_E + \left\|\mathbf{e}_u^n, \mathbf{e}_\sigma^{n+\frac{1}{2}}\right\|_E\right)$$
$$\times \left(\left\|\frac{\partial \mathbf{u}^{n+\frac{1}{2}}}{\partial t} - \delta_t \mathcal{I} \mathbf{u}^{n+\frac{1}{2}}\right\|_\rho + \left\|\frac{\partial \boldsymbol{\sigma}^{n+1}}{\partial t} - \delta_t \mathcal{J} \boldsymbol{\sigma}^{n+1}\right\|_A\right). \tag{77}$$

Divide both sides by $\left\|\mathbf{e}_u^{n+1}, \mathbf{e}_\sigma^{n+\frac{3}{2}}\right\|_E + \left\|\mathbf{e}_u^n, \mathbf{e}_\sigma^{n+\frac{1}{2}}\right\|_E$, and summing from $n = 0$ to $N-1$,

$$\left\|\mathbf{e}_u^N, \mathbf{e}_\sigma^{N+\frac{1}{2}}\right\|_E \leq \left\|\mathbf{e}_u^0, \mathbf{e}_\sigma^{\frac{1}{2}}\right\|_E$$
$$+ K\Delta t \sum_{n=0}^{N-1}\left(\left\|\frac{\partial \mathbf{u}^{n+\frac{1}{2}}}{\partial t} - \delta_t \mathcal{I} \mathbf{u}^{n+\frac{1}{2}}\right\|_\rho + \left\|\frac{\partial \boldsymbol{\sigma}^{n+1}}{\partial t} - \delta_t \mathcal{J} \boldsymbol{\sigma}^{n+1}\right\|_A\right). \tag{78}$$

Note that using the interpolation properties in Lemmas 2 and 4,

$$\left\|\frac{\partial \mathbf{u}^{n+\frac{1}{2}}}{\partial t} - \delta_t \mathcal{I} \mathbf{u}^{n+\frac{1}{2}}\right\|_\rho \leq \left\|\frac{\partial \mathbf{u}^{n+\frac{1}{2}}}{\partial t} - \delta_t \mathbf{u}^{n+\frac{1}{2}}\right\|_\rho + \left\|\delta_t \mathbf{u}^{n+\frac{1}{2}} - \delta_t \mathcal{I} \mathbf{u}^{n+\frac{1}{2}}\right\|_\rho$$
$$\leq K\left(\Delta t^2 \left|\mathbf{u}^{n+\frac{1}{2}}\right|_{W^{2,\infty}(0,T;L^2(\Omega)^d)} + h^{k+1}\left|\frac{\partial}{\partial t}\mathbf{u}^{n+\frac{1}{2}}\right|_{H^{k+1}(\Omega)^d}\right). \tag{79}$$

Similarly,

$$\left\|\frac{\partial \boldsymbol{\sigma}^{n+1}}{\partial t} - \delta_t \mathcal{J} \boldsymbol{\sigma}^{n+1}\right\|_A \leq K\left(\Delta t^2 \left|\boldsymbol{\sigma}^{n+\frac{1}{2}}\right|_{W^{2,\infty}(0,T;L^2(\Omega)^{d\times d})} + h^{k+1}\left|\frac{\partial}{\partial t}\boldsymbol{\sigma}^{n+1}\right|_{H^{k+1}(\Omega)^{d\times d}}\right). \tag{80}$$

The result follows from (78)–(80) as $N\Delta t \leq T$. □

6. Numerical results

In this section, we present some numerical results to validate our new method. We show numerically that the scheme has the optimal rate of convergence and has a superconvergent property for dispersion error. We also present an application of the method to Rayleigh wave propagation.

We consider the two-dimensional case, i.e. $d = 2$. We will consider only rectangular domain that can be divided into squares. We subdivide each of the squares into two triangles. We use these triangles as our initial mesh. Therefore the staggered mesh can be viewed as a repetition of a square cell, which is shown in Fig. 2. We define the mesh size h as the side length of the square cell. To begin with, we compute the stability constant $\widetilde{K}_C$ for this mesh. We note that the P-wave velocity v_p is larger than the S-wave velocity v_s and the constant $\widetilde{K}_C$ is proportional to v_p^{-1}. By computing the constant numerically, we find that

$$\widetilde{K}_C \approx \begin{cases} 0.0962\, v_p^{-1}h, & \text{for } k = 1, \\ 0.0543\, v_p^{-1}h, & \text{for } k = 2. \end{cases}$$
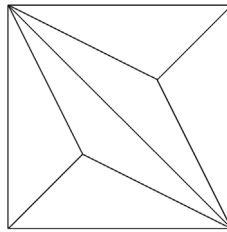
Fig. 2. A cell in the structured mesh with mesh size h.

Table 1
Convergence history

$1/h$	$\|(\mathbf{u}_h)_1 - u_1\|_\rho$	Order	$\|(\mathbf{u}_h)_2 - u_2\|_\rho$	Order	$\|\boldsymbol{\sigma}_h - \boldsymbol{\sigma}\|_\mathbf{A}$	Order
	$k = 1, \Delta t = 1/320{,}000$					
2	2.1408e+00	–	2.4847e+00	–	3.2472e+00	–
4	2.4265e−01	3.14	3.4899e−01	2.83	5.4482e−01	2.58
8	4.9326e−02	2.30	7.7508e−02	2.17	1.2632e−01	2.11
16	1.1568e−02	2.09	1.8914e−02	2.03	3.1163e−02	2.02
32	2.8410e−03	2.03	4.6984e−03	2.01	7.7821e−03	2.00
64	7.0947e−04	2.00	1.1735e−03	2.00	1.9443e−03	2.00
	$k = 2, \Delta t = 1/640{,}000$					
1	2.4234e+00	–	2.8755e+00	–	3.6994e+00	–
2	4.4169e−01	2.46	3.8183e−01	2.91	5.7887e−01	2.68
4	1.2946e−02	5.09	1.9008e−02	4.33	3.2533e−02	4.15
8	1.4950e−03	3.11	2.2950e−03	3.05	3.9442e−03	3.04
16	1.8182e−04	3.04	2.8348e−04	3.02	4.9213e−04	3.00
32	2.3040e−05	2.98	3.7648e−05	2.91	6.2917e−05	2.97

Table 2
Comparison of dispersion between our SDG scheme and a fourth order FD scheme. The density ρ, the velocities v_p and v_s are 1500, 520 and 52 respectively. The wave numbers k_x and k_z are taken as $\sqrt{2/3}$ and $\sqrt{1/3}$ respectively.

	The SDG scheme ($k = 1$)				Fourth order FD scheme			
$1/h$	Error of ω_1	Order	Error of ω_2	Order	Error of ω_1	Order	Error of ω_2	Order
1	1.2721e−02	–	2.9937e−04	–	3.0075e−03	–	3.0075e−03	–
2	6.4056e−04	4.31	1.8890e−05	3.99	1.9348e−04	3.96	1.9348e−04	3.96
4	2.3849e−05	4.75	1.1836e−06	4.00	1.2178e−05	3.99	1.2178e−05	3.99
8	2.4370e−06	3.29	7.4016e−08	4.00	7.6249e−07	4.00	7.6249e−07	4.00
16	1.4212e−07	4.10	4.6892e−09	3.98	4.7677e−08	4.00	4.7677e−08	4.00
32	8.7742e−09	4.02	1.2171e−10	5.27	2.9800e−09	4.00	2.9739e−09	3.66
	The SDG scheme ($k = 2$)				Fourth order FD scheme			
0.5	2.7897e−03	–	3.7089e−05	–	4.2526e−02	–	4.2526e−02	–
1	2.8064e−05	6.64	6.3004e−07	5.88	3.0075e−03	3.82	3.0075e−03	3.82
2	3.1291e−07	6.49	1.0163e−08	5.95	1.9348e−04	3.96	1.9348e−04	3.96
4	5.5620e−09	5.81	1.6672e−10	5.93	1.2178e−05	3.99	1.2178e−05	3.99
8	8.4232e−11	6.05	1.8254e−12	6.51	7.6249e−07	4.00	7.6249e−07	4.00

Example 1 (*Convergence Test*). We will test the convergence rate of our hybridized SDG method. We take $\Omega = [-15, 15]^2$ and $T = 0.02$. In addition, the density ρ, the P-wave velocity v_p and the S-wave velocity v_s are 1500, 520 and 300 respectively, where $\lambda + 2\mu = \rho v_p^2$ and $\mu = \rho v_s^2$. The initial conditions are $\mathbf{u}(0, x) = \exp(-2|x|^2)$ and $\boldsymbol{\sigma}(0, x) = \mathbf{0}$ and the source term $\mathbf{f} = \mathbf{0}$. For the comparison purpose, we compute a reference solution by using a fourth order locking-free finite difference scheme with a very fine mesh. For the SDG solution, we consider piecewise linear and quadratic approximations, that is, $k = 1$ and $k = 2$, and we will choose a fixed time step size Δt. In Table 1, we present the convergence history with weighted L^2 norms $\|u\|_\rho^2 = \int_\Omega \rho u^2 \, dx$ and $\|\boldsymbol{\sigma}\|_\mathbf{A}^2 = \int_\Omega \mathbf{A}\boldsymbol{\sigma} : \boldsymbol{\sigma} \, dx$. We see that optimal convergence rate is obtained. We remark that the Poisson ratio for this problem is 0.251. We tested a case with Poisson ratio 0.495 and obtained similar results.

Example 2 (*Dispersion Error*). We follow the eigenvalue method used in [25] for acoustic and electromagnetic wave equations. Let $d = 2$. We consider a structured mesh generated by repetition of a square cell, which is shown in Fig. 2. Then we consider the scheme given by (15)–(18) with $\mathbf{f} = \mathbf{0}$. Assume the solutions are plane waves given by $e^{-i(\mathbf{k}\cdot\mathbf{x}-\omega t)}$ where $\mathbf{k} = (k_x, k_z)$ is the wave number and ω is the frequency. Taking time derivatives in (15) and use (16)–(18) to eliminate
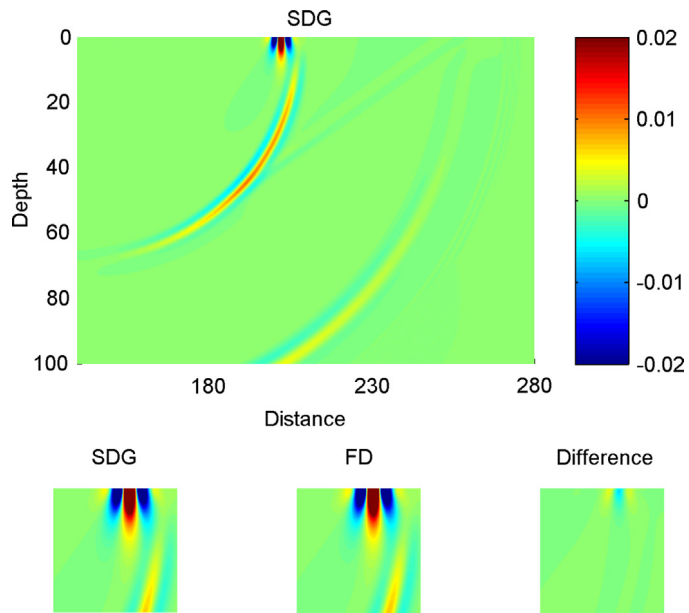
Fig. 3. The velocity u_2 at time $t = 0.25$ s. The upper figure is the solution of our SDG method. The lower three figures are the SDG solution, the fourth-order FD reference solution and the difference (6.5%) of them around the Rayleigh wave. All these figures are displayed with the same color axis.
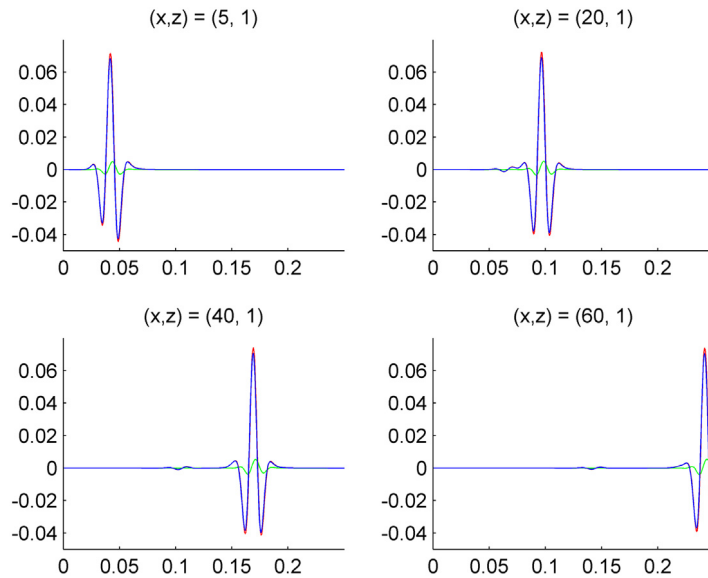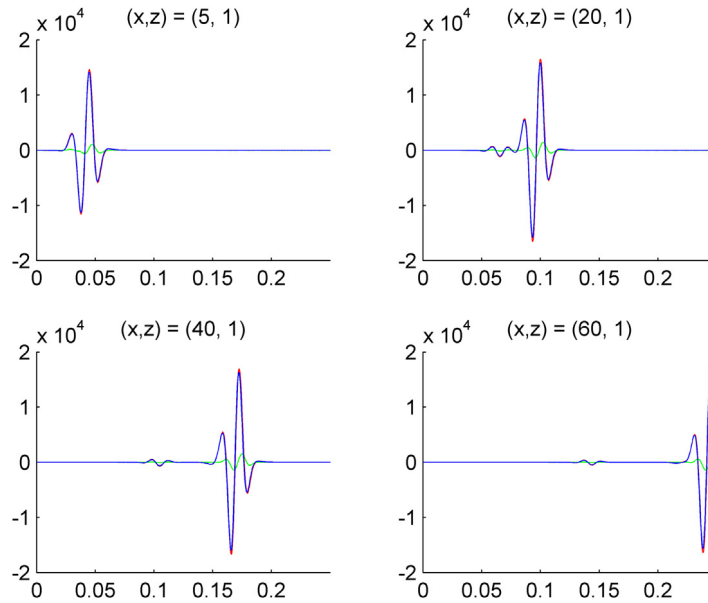

Fig. 4. The velocity u_2 at various points in the example of Lamb's problem. The horizontal and vertical axes stand for the time and the magnitude. The red curve and the blue curve are the solution of u_2 of the finite difference scheme and the SDG method respectively, while the green curve is the difference between these two solutions. Here x is the distance while z is the depth. (For interpretation of the references to colour in this figure legend, the reader is referred to the web version of this article.)

other variables, we obtain a linear system of the form

$$\mathbf{A}_1 \mathbf{U}_{tt} = \mathbf{A}_2 \widetilde{\mathbf{U}}, \tag{81}$$

where $\mathbf{U}$ is the vector representing the nodal values of $\mathbf{u}$ in the cell and $\widetilde{\mathbf{U}}$ is the vector representing the nodal values of $\mathbf{u}$ that $\mathbf{U}$ is depending on. We substitute $u_j = \alpha_j(\mathbf{x})e^{-i(\mathbf{k}\cdot\mathbf{x} - \omega_h t)}, j = 1, 2$, in this equation, we obtained a generalized eigenvalue problem:

$$\omega_h^2 \widetilde{\mathbf{A}} \boldsymbol{\eta} - \widetilde{\mathbf{A}}_2 \boldsymbol{\eta}.$$

Fig. 5. The stress σ_{11} at various points in the example of Lamb's problem. The horizontal and vertical axes stand for the time and the magnitude respectively. The red curve and the blue curve are the solution of σ_{11} of the finite difference scheme and the SDG method respectively, while the green curve is the difference between these two solutions. (For interpretation of the references to colour in this figure legend, the reader is referred to the web version of this article.)

It is well-known that the angular frequencies for P-wave and S-wave, namely, ω_1 and ω_2 are given by

$$\omega_1^2 = \frac{1}{\rho}(\lambda + 2\mu)(k_x^2 + k_z^2) \quad \text{and} \quad \omega_2^2 = \frac{1}{\rho}\mu(k_x^2 + k_z^2), \tag{82}$$

where k_x and k_z are the wave numbers in x and z direction respectively. We define the dispersion error for ω_1 and ω_2 as

$$\min_{\omega_h} \left| \frac{\omega_j^2}{\omega_h^2} - 1 \right|.$$

Table 2 shows the dispersion error for materials with high Poisson's ratio, 0.495. We can see that the proposed SDG scheme obtains a fourth order convergence when $k = 1$ and obtains a six order convergence when $k = 2$, which are two orders higher than dispersion errors for fully discrete non-staggered methods [26]. In [27], Ainsworth proved that the semi-discrete dispersion error of non-staggered DG methods matches these results reported for our method for upwind fluxes. However, our staggered hybridized method improves these rates by one order compared to semi-discrete non-staggered DG with central fluxes.

Example 3 (*Lamb's Problem*). We will test our method by the Lamb's problem [28], which is a classical test case for the implementation of free surface boundary condition. The problem setting is as follows. The density, the velocity for the P-wave and S-wave are 1500, 520, 300 respectively and the corresponding Poisson's ratio is 0.251. The computation domain is $[0, 280] \times [0, 140]$ and the free surface is set at depth $z = 0$. A vertical point force is applied to the free surface at $(x, z) = (140, 0)$. The force is given by a Ricker wavelet defined by the first derivative of

$$w(t) = 2\pi f(t - t_0)e^{-\pi^2 f^2(t-t_0)^2},$$

where the frequency $f = 50$ and $t_0 = 0.024$.

The solution of the Lamb's problem can be computed analytically [29]. For convenience, we compare our result to the solution given by a fourth-order finite difference scheme on a finer mesh. The SDG solution is computed with mesh size $h = 0.25$ while the FD solution is computed with mesh size $h = 0.1$. In Fig. 3, the upper figure is the SDG solution of u_2 at $t = 0.25$ in $[140, 280] \times [0, 100]$. The lower three figures are the SDG solution in $[190, 210] \times [0, 20]$, the FD solution in the same region, and their difference, respectively. There is only 6.5% difference in the small region. In Fig. 4, we show the SDG and FD solutions for the velocity u_2 and their differences at various locations from $t = 0$ to 0.25. In Fig. 5, we do the same for the stress σ_{11}. These results show our SDG method produces accurate solutions for the Lamb's problem.

7. Conclusion

In this paper, we have developed and analyzed a new staggered hybridization technique for the DG approximation for the elastic wave equations (2) and (3). The method is optimally convergent, numerically stable, locally and globally energy conserving and locking-free. Besides, the numerical stress tensor is strongly symmetric. Numerical results have also shown that this method has the super-convergence property for the dispersion error.

Acknowledgments

References

[1] Alan R. Levander, Fourth-order finite-difference P-SV seismograms, Geophysics 53 (11) (1988) 1425–1436.
[2] Raul Madariaga, Dynamics of an expanding circular fault, Bull. Seismol. Soc. Am. 66 (3) (1976) 639–666.
[3] Jean Virieux, P-SV wave propagation in heterogeneous media: Velocity–stress finite-difference method, Geophysics 51 (4) (1986) 889–901.
[4] V. Etienne, E. Chaljub, J. Virieux, N. Glinsky, An hp-adaptive discontinuous Galerkin finite-element method for 3-D elastic wave modelling, Geophys. J. Int. 183 (2) (2010) 941–962.
[5] Leszek Demkowicz, J.T. Oden, Application of hp-adaptive BE/FE methods to elastic scattering, Comput. Methods Appl. Mech. Engrg. 133 (3) (1996) 287–317.
[6] Lucas C. Wilcox, Georg Stadler, Carsten Burstedde, Omar Ghattas, A high-order discontinuous Galerkin method for wave propagation through coupled elastic–acoustic media, J. Comput. Phys. 229 (24) (2010) 9373–9396.
[7] P.J. Matuszyk, L.F. Demkowicz, C. Torres-Verdín, Solution of coupled acoustic-elastic wave propagation problems with anelastic attenuation using automatic hp-adaptivity, Comput. Methods Appl. Mech. Engrg. 213 (2012) 299–313.
[8] P.F. Antonietti, I. Mazzieri, A. Quarteroni, F. Rapetti, Non-conforming high order approximations of the elastodynamics equation, Comput. Methods Appl. Mech. Engrg. 209212 (2012) 212–238.
[9] Jonás D. De Basabe, Mrinal K. Sen, Mary F. Wheeler, The interior penalty discontinuous Galerkin method for elastic wave propagation: grid dispersion, Geophys. J. Int. 175 (1) (2008) 83–93.
[10] Béatrice Rivière, Simon Shaw, Mary F. Wheeler, J.R. Whiteman, Discontinuous Galerkin finite element methods for linear elasticity and quasistatic linear viscoelasticity, Numer. Math. 95 (2) (2003) 347–376.
[11] Appelö Daniel, Thomas Hagstrom, A new discontinuous Galerkin formulation for wave equations in second-order form, SIAM J. Numer. Anal. 53 (6) (2015) 2705–2726.
[12] Sarah Delcourte, Loula Fezoui, Nathalie Glinsky-Olivier, A high-order discontinuous Galerkin method for the seismic wave propagation, in: ESAIM: Proceedings, vol. 27, EDP Sciences, 2009, pp. 70–89.
[13] N.C. Nguyen, J. Peraire, B. Cockburn, High-order implicit hybridizable discontinuous Galerkin methods for acoustics and elastodynamics, J. Comput. Phys. 230 (10) (2011) 3695–3718.
[14] Martin Käser, Michael Dumbser, An arbitrary high-order discontinuous Galerkin method for elastic waves on unstructured meshes I. The two-dimensional isotropic case with external source terms, Geophys. J. Int. 166 (2) (2006) 855–877.
[15] Eric T Chung, Björn Engquist, Optimal discontinuous Galerkin methods for wave propagation, SIAM J. Numer. Anal. 44 (5) (2006) 2131–2158.
[16] Eric T Chung, Björn Engquist, Optimal discontinuous Galerkin methods for the acoustic wave equation in higher dimensions, SIAM J. Numer. Anal. 47 (5) (2009) 3820–3848.
[17] Eric T Chung, Chi Yeung Lam, Jianliang Qian, A staggered discontinuous Galerkin method for the simulation of seismic waves with surface topography, Geophysics 80 (4) (2015) T119–T135.
[18] Eric Chung, Bernardo Cockburn, Guosheng Fu, The staggered DG method is the limit of a hybridizable DG method, SIAM J. Numer. Anal. 52 (2) (2014) 915–932.
[19] Bernardo Cockburn, Jayadeep Gopalakrishnan, Raytcho Lazarov, Unified hybridization of discontinuous Galerkin, mixed, and continuous Galerkin methods for second order elliptic problems, SIAM J. Numer. Anal. 47 (2) (2009) 1319–1365.
[20] Bernardo Cockburn, Vincent Quenneville-Bélair, Uniform-in-time superconvergence of the HDG methods for the acoustic wave equation, Math. Comp. 83 (285) (2014) 65–85.
[21] Weifeng Qiu, Jiguang Shen, Ke Shi, An HDG method for linear elasticity with strong symmetric stresses, ArXiv Preprint ArXiv:1312.1407 (2013).
[22] Bernardo Cockburn, Ke Shi, Superconvergent HDG methods for linear elasticity with weakly symmetric stresses, IMA J. Numer. Anal. 33 (3) (2013) 747–770.
[23] Jeonghun J. Lee, Hyea Hyun Kim, Analysis of a staggered discontinuous Galerkin method for linear elasticity, J. Sci. Comput. (2015) 1–25.
[24] Hiu Ning Chan, Eric T. Chung, Gary Cohen, Stability and dispersion analysis of the staggered discontinuous Galerkin method for wave propagation, Internat. J. Numer. Anal. Model. 10 (1) (2013).
[25] Gary Cohen, Higher-Order Numerical Methods for Transient Wave Equations, Springer, 2002.
[26] D. Sármány, M.A. Botchev, J.J.W. van der Vegt, Dispersion and dissipation error in high-order Runge-Kutta discontinuous Galerkin discretisations of the Maxwell equations, J. Sci. Comput. 33 (1) (2007) 47–74.
[27] Mark Ainsworth, Dispersive and dissipative behaviour of high order discontinuous Galerkin finite element methods, J. Comput. Phys. 198 (1) (2004) 106–130.
[28] Horace Lamb, On the propagation of tremors over the surface of an elastic solid, Phil. Trans. R. Soc. Lond. Ser. A (1904) 1–42.
[29] A.T. De Hoop, A modification of cagniards method for solving seismic pulse problems, Appl. Sci. Res. B 8 (1) (1960) 349–356.